JOURNAL OF GEOPHYSICAL RESEARCH, VOL. 87, NO. A1, PAGES 17–34, JANUARY 1, 1982

Nonlocal Plasma Turbulence Associated With Interplanetary Shocks

C. F. KENNEL[1], F. L. SCARF, AND F. V. CORONITI[2]

Space Sciences Department, TRW Defense and Space Systems Group, Redondo Beach, California 90278

E. J. SMITH

Jet Propulsion Laboratory, California Institute of Technology, Pasadena, California 91109

D. A. GURNETT

Department of Physics and Astronomy, University of Iowa, Iowa City, Iowa 52242

The plasma wave instrument on ISEE 3 has detected regions of plasma turbulence that extend several tenths of an astronomical unit upstream or downstream of inteplanetary shocks. The plasma waves fall into four categories. Highly impulsive 1- 10-kHz electric field bursts were found hours upstream of quasi-parallel interplanetary shocks. On occasion their average and peak amplitudes increased monotonically until the shock crossing, at which time they were suppressed. A lower frequency electric field (0.1–1 kHz) component was enhanced at nearly all shocks and persisted downstream. Broadband low-frequency (typically <178 Hz) magnetic fluctuations increased at, and persisted hours downstream of, every interplanetary shock in our sample. A smooth high-frequency continuum, near and above the local electron plasma frequency, was enhanced at, and persisted well downstream of, every interplanetary shock we studied. Impulsive electron plasma wave bursts were occasionally found near the shocks. The shock-associated plasma waves we found to extend over large spatial scales are similar to those found previously in local studies of interplanetary shocks. While no single interplanetary shock showed every effect, the ensemble of shocks contained at least one example of each type of plasma wave found upstream of the earth's bow shock. The 1- to 10-kHz spectra upstream of interplanetary shocks and the earth's bow shock are similar. The low-frequency electric and magnetic fluctuations downstream of interplanetary shocks and the bow shock have similar spectra. They seem to be ubiquitous features of flowing plasmas made turbulent by a shock.

1. INTRODUCTION

Extended regions of plasma wave turbulence are associated with the passage of interplanetary shocks over ISEE 3. The plasma waves in four characteristic frequency ranges behave in different ways. The four ranges are high frequency ($\geq$10 kHz) electric fields, intermediate frequency (1–10 kHz) electric fields, low-frequency (0.1–1 kHz) electric fields, and low frequency (3–178 Hz) magnetic fields. They can be observed hours before or after a shock and thus can extend up to a tenth of an astronomical unit on either side of the discontinuity. These wave measurements reflect the plasma conditions created in the solar wind by the shock, its piston, and ensuing rarefaction zone, as well as those in the thin shock dissipation layer. The low-frequency electric and magnetic fluctuations resemble those in the magnetosheath downstream of the earth's bow shock, and the 1- to 10 kHz electric field spectra upstream of the bow shock and interplanetary shocks are similar.

Although this paper addresses only the microscopic plasma waves associated with interplanetary shocks, we attempt to place our preliminary study in a broad context by discussing some potential contributions to collisionless shock and cosmic ray acceleration theories by amplification of the line of research proposed here.

Most experimental information about collisionless shock structure comes from the earth's bow shock. Synthesis of detailed case studies has led to a classification of shock structure according to upstream flow parameters that has a firm basis in theory [*Greenstadt,* 1976; *Formisano,* 1977]. Statistical and case studies have clarified the phenomenology of the region of disturbance upstream of the bow shock, a subject discussed by *Greenstadt and Fredricks* [1979] and in a special issue of *Journal of Geophysical Research* (vol. 86). We now review these interrelated topics briefly to relate our present study of interplanetary shocks to overall shock theory.

The very discovery of the bow shock [*Ness et al.,* 1964] was called into question by uncertainty whether it was thin or thick—a 'broad disordered transition' [*Bernstein et al.,* 1964; *Scarf et al.,* 1965]. The discovery issue was settled by detailed OGO 5 studies of local shock structure [*Fredricks et al.,* 1968, 1970]. Many of the clearest events studied by OGO 5 and other early spacecraft were quasi-perpendicular shocks, which we now know to be easily identifiable. In retrospect, our early difficulties with shock identification arose because we were unaware of how parameter-sensitive collisionless shock structure really is. Bow shock structure depends upon the upstream ratio of thermal to magnetic energy density β, upon the Mach number, and upon the magnetic shock normal angle θ_{Bn}. Magnetic turbulence upstream, and especially downstream, increases with increasing upstream β. Ions are strongly heated and may be reflected from an electrostatic subshock, above a critical fast

[1] Also at Department of Physics and Institute of Geophysics and Planetary Physics, University of California, Los Angeles, California 90024.

[2] Also at Department of Physics and Department of Astronomy, University of California, Los Angeles, California 90024.

Paper number 1A1472.
0148-0227/82/001A-1472$01.00

Mach number of about 2.5 [*Formisano,* 1977]. θ_{Bn} is the most critical controlling parameter. Quasi-perpendicular shocks, with $\theta_{Bn} > 50°$, are thin and well-defined. By contrast, quasi-parallel shocks, with $\theta_{Bn} \lesssim 50°$, have such broad regions of magnetic disorder that it has proven difficult to identify a thin magnetic shock jump, and not much is known about the quasi-parallel density jumps. Quasi-perpendicular shock structure is well understood below the critical Mach number [*Galeev,* 1976], and quasi-perpendicular bow shocks dominate the published case studies because of their easy identifiability. However, supercritical quasi-parallel shocks are an important fraction of the bow shocks encountered.

As early as 1968, we knew that an element of solar wind flow could have foreknowledge of an impending bow shock crossing if it were connected magnetically to the shock [*Anderson,* 1968, 1969; *Fairfield,* 1969]. Because the interplanetary field is intrinsically variable and is made even more unsteady by its connection to the shock, the next decade was needed to deduce the spatial structure described below of an ideal foreshock in a steady solar wind [*Greenstadt and Fredricks,* 1979]. The interplanetary magnetic field line instantaneously tangent to the bow shock surface defines the leading edge of the foreshock. The shock is locally perpendicular at the point of tangency. Electrons and ions acquire several keV energy near the point of tangency. *Sonnerup* [1969] suggested they gain energy from the solar wind electric field by multiple reflection from the shock surface. These accelerated particles propagate upstream parallel to the magnetic field in flux tubes that are swept downstream at the electric field drift speed of the solar wind. Reflected electrons are, therefore, found downstream of the instantaneously tangent interplanetary field line and upstream of reflected ions of the same energy. The leading edges of the reflected electron and ion zones contain few keV beams moving parallel to the magnetic field [*Anderson,* 1968, 1969; *Anderson et al.,* 1981; *Gosling et al.,* 1978]. The superthermal electron and ion distributions become progressively more diffuse with increasing distance downstream from the beam leading edges [*Anderson et al.,* 1979; *Gosling et al.,* 1978; *Greenstadt et al.,* 1980]. Nonetheless, the superthermal ion and electron energy fluxes still appear to be directed away from the shock. Because the bow shock is curved, the magnetic field connects the diffuse particle zones to quasi-parallel shocks. Large amplitude hydromagnetic waves are found in the diffuse proton zone [*Paschmann et al.,* 1979; *Greenstadt et al.,* 1980; *Hoppe et al.,* 1981]. In addition, whistler waves [*Fairfield,* 1974; *Anderson et al.,* 1981; *Hoppe et al.,* 1981], electron plasma oscillations [*Scarf et al.* 1971; *Anderson et al.,* 1981], and ion acoustic waves [*Scarf et al.,* 1970; *Rodriquez and Gurnett,* 1975; *Anderson et al.,* 1981] are found upstream on bow shock-connected field lines.

While there is general agreement about the upstream phenomenology outlined above, there are differences of opinion about its physical interpretation and about those detailed measurements that bear on one or another interpretation. The central issues are the origin of the diffuse ions that connect magnetically to the quasi-parallel zone of the bow shock, and their relationship to upstream magnetic turbulence. It has been argued [*Bame et al.,* 1980] that many, and perhaps most, of the upstream ions are generated where the bow shock is quasi-perpendicular and originally are part of the ion foreshock beam. As beam ions move upstream, they become unstable to the growth of electromagnetic waves. They subsequently pitch angle scatter and lose parallel momentum to the waves that ultimately deposit it in the solar wind. Decelerated ions and waves that cannot propagate at the solar wind speed are blown downstream to fill the region downstream of the ion foreshock with superthermal ions and waves. The superthermal ion distributions do change from beamlike to diffuse with increasing distance downstream from the foreshock, with intermediate distributions between [*Gosling et al.,* 1978; *Greenstadt et al.,* 1980]. There is no doubt that the observed foreshock beam distributions are unstable [*Gary,* 1981; *Sentman et al.,* 1981*b*], and it is reasonable to argue that intermediate distributions evolve from beams. Moreover, the solar wind is deflected by an amount roughly compatible with momentum loss from upstream ions [*Bonifazi et al.,* 1980]. However, because the foreshock beams are thin spatial structures, and the solar wind rest-frame diffuse ion heat flux, integrated over the area of outflow [*Sentman et al.,* 1981*a*], is comparable with the power dissipated in a small substorm, one can question whether all the diffuse ions come from the foreshock beam, especially since some of the heat generated in quasi-parallel shocks might escape upstream. Without measurements of the entire ion beam energy and number flux near the beam acceleration point, it is difficult to settle this issue quantitatively.

It is important to collisionless shock theory to understand whether the upstream diffuse ions come from the ion foreshock beam or the quasiparallel bow shock. If they originate in the foreshock beam, one could argue that, since the magnetic turbulence created by the beam instability is blown into the shock, the observed disordered quasi-parallel structure is an artifact of the small radius of curvature of the bow shock. In other words, a plane quasi-parallel shock could be intrinsically thin. On the other hand, if many diffuse upstream ions are generated by the quasi-parallel shock, such shocks could be inherently thick, since the measured diffuse ions are also unstable [*Sentman et al,* 1981*b*] to hydromagnetic waves.

Studying bigger shocks could help resolve the intrinsic structure of quasi-parallel shocks. Since the ratio of shock radius of curvature to intrinsic plasma scale lengths is 250–2500 times larger for interplanetary shocks than for the bow shock, interplanetary shocks are of interest from the above point of view. However, detections of the classical upstream signatures—superthermal ions and magnetohydrodynamic waves—hours before a shock crossing have been difficult to relate to the shock, not only because the solar wind normally has energetic ions and is magnetically turbulent, but also because the shock and interplanetary field geometry is difficult to ascertain. Our increasingly complete understanding of bow shock upstream phenomenology can help clarify the shock association. MHD turbulence that is accompanied by other upstream signatures could then be plausibly related to the shock. This paper is a first step in this program. Since plasma waves are sensitive to deviations from thermal equilibrium, they might provide an early indicator of an impending shock crossing.

The region downstream of shocks is of equal interest to that upstream. For instance, one parallel high-β shock theory [*Kennel and Sagdeev,* 1967], predicts that large-amplitude Alfvén waves created at the shock should persist

well downstream. Indeed, the magnetosheath downstream of the quasi-parallel bow shock is more turbulent magnetically than that downstream of the quasi-perpendicular zone [*Formisano,* 1977]. *Olson et al.* [1969] first discussed the broadband spectrum of magnetic fluctuations above the proton gyrofrequency downstream of the bow shock. Helios 1 found similar magnetic noise immediately downstream of selected interplanetary shocks [*Neubauer et al.,* 1977; *Gurnett et al.,* 1979]. *Rodriguez and Gurnett* [1975] and *Rodriguez* [1979] have found that 0.1- to 1-kHz electric field fluctuations are characteristic of the postshock magnetosheath. Since the magnetosheath is turbulent when it hits the magnetopause, the bow shock may not be completely separated from its piston, in that the plasma has not relaxed completely to its downstream equilibrium state. To study the relaxation process, magnetosheath data far downstream from the earth would be needed, which could be contaminated by particles escaping from the magnetosphere. Since the separations between interplanetary shocks and their pistons is larger in basic plasma units than that between the bow shock and the magnetopause, studies of interplanetary shocks may help clarify how strong shocks relax downstream. A complete account of shock structure should thus include the extended dissipation regions upstream and downstream of the shock. Bow shock studies have not measured their true extent. For example, we have not systematically probed the region upstream of the bow shock beyond the orbit of the moon, and until ISEE 3, most spacecraft studies of it were limited to orbital apogees of 30 R_E of less. Although they are not suited for investigations of local quasi-perpendicular shock structure, interplanetary shocks are a convenient means to study nonlocal shock effects, since the entire structure moves over the spacecraft.

Table 1 in section 2 lists the parameters of the shocks to be studied in this paper. The list contains both quasi-parallel and quasi-perpendicular shocks and emphasizes higher Mach number shocks that are more directly comparable to the bowshock. We also survey the behavior of the intermediate and low-frequency electric fields and the low-frequency magnetic field by assembling the data from three frequency bands for six sample shocks. There follow more detailed case studies of individual shocks. The shock events of November 11 and 12, 1978 (section 3), and April 4–5, 1979 (section 4), are similar. Both are super-critical quasi-parallel shocks, with fast Mach numbers of 4.7 and 2.9, and θ_{Bn} of 22° and 43.5°, respectively. Both may have similar drivers. Observations of bi-directional electron streaming in the helium-enriched solar flare plasma that followed the November 12, 1978, shock indicate that its driver was contained in a low-β closed magnetic field structure [*Bame et al.,* 1981]. A large scale rotation of the magnetic field beginning nine hours after the April 5, 1979, shock suggests that its driver may have been similar. The shock events of April 24–25, 1979 (section 5), and June 6–7, 1979 (section 6), may have been driven by corotating fast streams. A forward-reverse shock pair was observed on April 24–25, 1979 (section 5), and June 6–7, 1979 (section 6), may have been driven by corotating fast streams. A forward-reverse shock pair was observed on April 24–25, and a possible developing reverse shock was observed on June 7. The solar wind speed reached 900 km/s downstream of the June 6 forward shock. Two successive forward shocks were observed on November 29–30, 1979 (section 6). The region between the shocks contained very little electric field noise, except for an enhanced continuum of electron plasma waves.

In section 7, we compare electric and magnetic spectra taken close to interplanetary shocks with those up and downstream of the bow shock. The spectra are quite similar. Moreover, the upstream interplanetary shock spectra appear to be organized by θ_{Bn} in the same way as bow shock spectra. Section 8 closes with a summary and discussion of our results.

Establishing the intrinsic structure of quasi-parallel shocks may prove important to the theory of cosmic ray acceleration by interplanetary and interstellar shocks. Shocks accelerate ions in several ways. Ions whose Larmor radius exceeds the shock thickness conserve their gyrophase-averaged magnetic moment [E. N. Parker, unpublished manuscript, 1958; *Chen and Armstrong,* 1972; *Shabanskii,* 1972; *Pesses,* 1979; *Terasawa,* 1979*a, b*]. Depending upon their pitch angle, upstream ions are either reflected by or transmitted through the shock. Reflected ions grad-B drift parallel to the flow electric field, and they acquire energy from the field more efficiently the more perpendicular the shock. However, since multiple reflections are needed to account for the observed acceleration by interplanetary shocks [*Pesses,* 1979], it is thought that reflected ions scatter from upstream MHD turbulence back towards the shock. They are either re-reflected or transmitted at their next shock encounter. Re-reflected particles can repeat the above cycle. Transmitted particles can be scattered by downstream MHD turbulence back towards the shock. Such particles are subject to Fermi acceleration by multiple reflections between up and downstream waves that convect approximately with the local flow speed. The integral spectrum for nonrelativistic particles Fermi-accelerated by infinite plane parallel shocks depends only upon the ratio of the up and downstream flow speeds [*Krimsky,* 1977; *Axford et al.,* 1977; *Bell,* 1978*a, b*; *Blandford and Ostriker,* 1978]. Because the spectral index calculated for strong shocks is close to the observed galactic cosmic ray index, supernova shocks are promising candidates to accelerate cosmic rays. This acceleration would occur in the quasi-parallel zones of the shock surfaces. These theories assume that the shocked plasma and the cosmic rays self-consistently generate the required MHD turbulence and thus rely on analogy with the bow shock.

Here we have considered cosmic rays as a fluid of test particles. However, E. N. Parker (unpublished manuscript, 1958) argued that cosmic rays should contribute to interstellar shock structure. *Wentzel* [1971] and *Axford et al.* [1977] included cosmic rays as a second fluid in the shock Rankine-Hugoniot relations. In these models, the cosmic ray flux, a free parameter, is conserved across the shock and, if it is large enough, can create a shock without a subshock in the thermal plasma. An energetic particle flux resides upstream prior to shock passage. *Eichler*'s [1979] kinetic model relates cosmic rays to the shocked thermal ions. Since the cosmic rays are accelerated out of the thermal plasma, their flux is determined as part of the shock structure solution. Strong shocks could dissipate as much as half their energy into cosmic rays.

Whether heated plasma ions create MHD turbulence as part of the quasi-parallel shock structure is an issue central to fully self-consistent cosmic ray acceleration theories. A qualitative combination [*Kennel,* 1981] of *Parker*'s [1961]

and *Kennel and Sagdeev*'s [1967] parallel shock theories suggests that it is possible. The proximity of the quasi-parallel and quasi-perpendicular zones obscures this issue at the bow shock. The shocks surrounding corotating interaction regions are too weak and too perpendicular to test the interstellar shock acceleration theory [*Eichler*, 1981]. *Eichler* [1981] has suggested that the 2327 UT August 4, 1972, solar flare shock [*Dryer et al.*, 1976] had an acceleration efficiency approaching that of interstellar shocks.

The above discussion of cosmic ray acceleration suggests that curved interplanetary shocks could have upstream regions structured similarly to that of the bow shock. Shock-reflected ions would be accelerated into field aligned distributions in the quasi-perpendicular zone of the shock surface. Well upstream, these ions would be found downstream of the interplanetary field line that is most nearly tangent to the shock surface. Further downstream, the field would connect to the quasi-parallel zone, where Fermi acceleration would operate. Of course, particles can diffuse to field lines whose connection to the shock is different, or the field can change its connection. *Pesses et al.* [1980] suggest that the quasi-parallel zone accelerates lower energy ions that act as seed particles for shock reflection acceleration. Overall acceleration to high energies would then be most efficient when changes in the interplanetary field cycle seed particles through the quasi-perpendicular reflection zone.

This paper uses ISEE 3 plasma wave measurements to establish two points. First, the microscopic plasma waves near interplanetary shocks, both upstream and downstream, are similar to those near the bow shock. Second, since the plasma waves extend large distances from interplanetary shocks, the plasma physics prevailing near the bow shock may apply to interplanetary shocks on a spatial scale large enough to be of interest to acceleration theories. Thus, by combining the highly resolved spatial and temporal measurements near the bow shock, with the greater ability to perceive the entire region of disturbance associated with interplanetary shocks, we may synthesize a picture useful to both collisionless shock and particle acceleration theories.

There have been numerous studies of the large scale hydromagnetic structure of interplanetary disturbances, many of which are preceded by shocks [*Burlaga et al.*, 1980; *Dryer et al.*, 1972; *Gosling et al.*, 1976; *Intriligator*, 1976; *Lazarus et al.*, 1970; *Schwenn et al.*, 1978, 1980; *Smith and Wolfe*, 1977, 1979; *Vaisberg and Zastenker*, 1976]. There have also been several studies of the plasma waves found near interplanetary shocks [*Scarf et al.*, 1971, 1974, 1981; *Scarf*, 1978; *Neubauer et al.*, 1977; *Gurnett et al.*, 1979; *Burlaga et al.*, 1980]. However, there have been relatively few that survey the plasma wave phenomenology throughout the entire event [e.g., *Burlaga et al.*, 1980], and none, to our knowledge, that survey upstream plasma waves from the point of view of the quasi-parallel, quasi-perpendicular distinction suggested by bow shock studies.

2. SURVEY OF SHOCK-ASSOCIATED PLASMA WAVE PHENOMENOLOGY

Table 1 displays parameters for the shocks studied in this paper. The upstream magnetic shock normal angle θ_{Bn}, the upstream β, and the fast Mach number M_F were calculated at JPL by using *Abraham-Schrauner and Yun*'s [1976] method, which uses plasma and magnetic field data immediately up and downstream of the shock discontinuity. In addition, we show the up and downstream number density, n_1 and n_2, in units of particles/cm^3; the up and downstream flow speeds, v_1 and v_2, in units of km/s; and the up and downstream magnetic field strength in units of 10^{-5} G, all taken from the common data pool. Since the data pool magnetic field is recorded every 64 s, and the density and flow speeds one-fifth as often, the data pool information cannot be used to compute shock normals, but the data set does indicate the plasma conditions prevailing a few minutes before and after a shock passage. Note that Table 1 contains both quasi-parallel and quasi-perpendicular, and sub- and super-critical, shocks.

Figure 1 presents 24 hours of plasma wave data surrounding six interplanetary shocks chosen to illustrate their variety. For typical shock speeds, 24 hours corresponds to a spatial scale of several tenths of an AU. Figure 1 shows observations in three frequency channels that the case studies to follow will show are representative: low-frequency magnetic fields and low and high frequency electric fields. Results from the channels corresponding to electron plasma oscillations will be discussed separately. The amplitudes are in logarithmic units; solid shading indicates the amplitudes averaged over 128 s, and dots indicate the peak amplitudes during the same interval. The magnetic field data are sampled 1/16 as often as the electric field. Further information about the plasma wave instrument is contained in *Scarf et al.*, 1978.

TABLE 1. Shock Parameters

Shock		JPL Shock Analysis			Common Data Pool Parameters					
Date	Time	θ_{Bn}	β_1	M_{F1}	n_1	n_2	v_1	v_2	B_1	B_2
Aug. 27, 1978	0211:20	42	3	3.3	8.3	39	310	425	4	10
Nov. 8, 1978	0110	51	0.45	2.3	13	30	350	430	12	20
Nov. 12, 1978	0028:16	22	0.51	4.7	6	14	370	680	8	18
Dec. 25, 1978	1118	88	1.5	1.65						
Jan. 9, 1979					12.3	38	382	460	.9	23
Feb. 3, 1979	1736	88	1.3	1.3	13	42	370	447	6.9	15.6
Feb. 21, 1979	0217	70	0.53	2.23	5	18	394	506	6.8	15.7
April 5, 1979	0120	44	0.21	2.9	8	28	430	559	13.3	29
April 24, 1979	2328	84.5	1.5	2.4	10	48	382	700	6	14.5
April 25, 1979	1250				18.5	4.5	580	660	25	16
May 29, 1979	1817	53	0.77	2.2	9.3	26.8	430	400	8.1	12.5
June 6, 1979	1842	26.1	1.26	3.16	27.5	112	308	461	13	36.6
Nov. 19, 1979	1539				18.7	35.8	290	308	2.9	4.8
Nov. 30, 1979	0648				34	99	299	371	8.3	21.2

The shocks may be located by the strong enhancements in the low frequency magnetic field. These shock identifications have been confirmed by interplanetary field data. Common to all six shocks in Figure 1, and all that we have identified, is the fact that the low-frequency magnetic fields persist many hours downstream. The two-hour enhancement following the shock on February 3, 1979, was the shortest we have found. At a nominal shock speed of 500 km/s, this corresponds to a distance of 0.02 AU or 500 R_E. All other disturbed regions were longer. The magnetic turbulence was confined between the forward and reverse shocks on April 24–25, 1979. The magnetic fluctuations behind the other shocks decreased with distance downstream and died out when the disturbances in the interplanetary field disappeared. On April 24, 1979, and February 3, 1979, low-frequency magnetic fluctuations did extend an hour upstream of the shocks, but they had lower amplitudes than those downstream. In most cases, the low-frequency magnetic channels gave no warning of an impending shock crossing.

We now turn to wave electric field measurements. The ISEE 3 plasma wave instrument generally records signals reliably in the 100 Hz–100 kHz frequency range. Above 10 kHz, these are usually associated with electron plasma oscillations and/or type III radio bursts. Two types of shock-associated behavior in the 100 Hz–10 kHz range are distinguishable by frequency. The low frequency, 100 Hz–1 kHz average amplitude was enhanced at the shock in all six cases in Figure 1. On August 27, 1979, November 8, 1978, and May 29, 1979, there were single sharp spikes of a few minutes duration. Since a shock crossing takes tenths of seconds, even these relatively small features are part of the nonlocal shock structure. On May 29, 1979, and April 24, 1979, the 311-Hz average amplitudes were enhanced downstream for several hours. On February 3, 1979, the enhanced amplitude persisted for at least an hour, until interference commencing at 1910 UT obscured the 311 Hz signal.

In none of the six cases were the average low frequency electric field amplitudes enhanced upstream of the shock. On the other hand, higher frequency signals did occur well upstream. Their large peak-to-average amplitude ratios indicate they were highly impulsive. Their behavior varied from shock to shock. Some shocks (November 7, 1978, and February 3, 1979) had little or no upstream enhancement; others (February 20, 1979, April 24, 1979, and May 24, 1979) had variable noise upstream, and the average amplitude increased more or less monotonically up to the August 27, 1978, shock. The few kHz electric fields, when they occurred, were found as much as 12 hours upstream. The few kHz peak and average electric field amplitudes maximized at all six shocks in Figure 1. The shocks marked a change in behavior from upstream to downstream. In the majority of cases (August 27, 1978, February 3, 1979, February 20, 1979, and April 24, 1979) the peak amplitudes were suppressed downstream. Upstream of the reverse shock on April 25, 1979, the peak few kHz electric field amplitudes were low; they increased downstream. This behavior is the reverse of that for forward shocks.

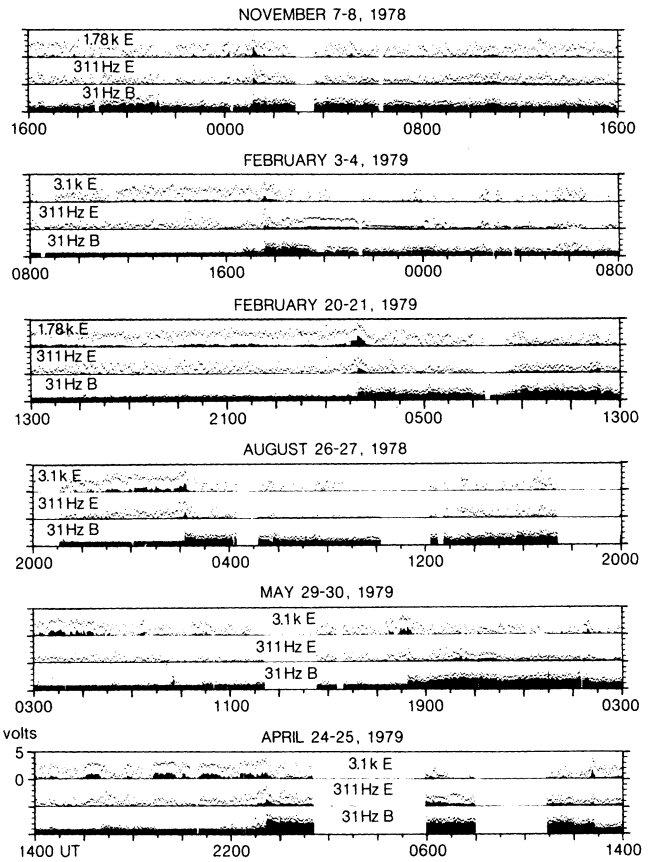

Fig. 1. Plasma waves associated with selected interplanetary shocks. We present 24 hours of plasma wave data, in three characteristic frequency channels, surrounding the passage of 6 interplanetary shocks over ISEE 3, chosen to reflect the variety of plasma wave phenomena we have encountered. The shock itself is most clearly identifiable in the 31-Hz magnetic field amplitude, which increases by at least an order of magnitude at each shock. This amplitude enhancement persists hours downstream of each shock. Note the foot or magnetic noise preceding the February 3, 1979, and April 24, 1979, shocks and that the enhanced magnetic noise was largely confined between the forward-reverse shock pair on April 24–25, 1979. Activity in the 1.78 kHz or 3.1-kHz electric field channels is probably due to Doppler-shifted ion acoustic noise. Note the extremely high ratio of 128-s peak (dots) to average (solid) amplitudes. The amplitudes are plotted logarithmically. This component is significantly more intense before the shock passage and tends to be suppressed downstream. It resumes after the 1250 UT reverse shock passage on April 25, 1979. The 311-Hz channel is representative of low-frequency electric field noise that is typically enhanced at the shock, especially in the average amplitude, and persists well downstream.

3. SHOCK EVENT OF NOVEMBER 11–12, 1978

Figure 2 shows eight channels of ISEE 3 electric field data and the interplanetary field magnitude for twelve hours surrounding the passage of an interplanetary shock at 0028 UT on November 12, 1978. Across the shock the solar wind speed jumped from 370 km/s to 680 km/s, the density from 4 cm^{-3} to 12 cm^{-3}, and the proton temperature from $3 \times 10^{4\circ}$K to $1.5 \times 10^{6\circ}$K [*Bame et al.*, 1981]. The upstream β was about 0.5. The shock normal vector **n** had the components in IS coordinates, $n_x = -0.957$, $n_y = 0.276$, $n_z = 0.093$, and the upstream magnetic field components were $B_{x1} = 6.40\gamma$, $B_{y1} = 0.99\gamma$, $B_{z1} = -3.23\gamma$, so that θ_{Bn} was 22°. The large negative B_{z1} suggests that ISEE 3 probably was not magnetically connected to the bow shock at 0028 UT. The shock speed was about 700 km/s; ISEE 1 detected it in the solar wind at 19 R_E geocentric distance at 0058 UT, a delay consistent with the estimated shock speed. The fast Mach

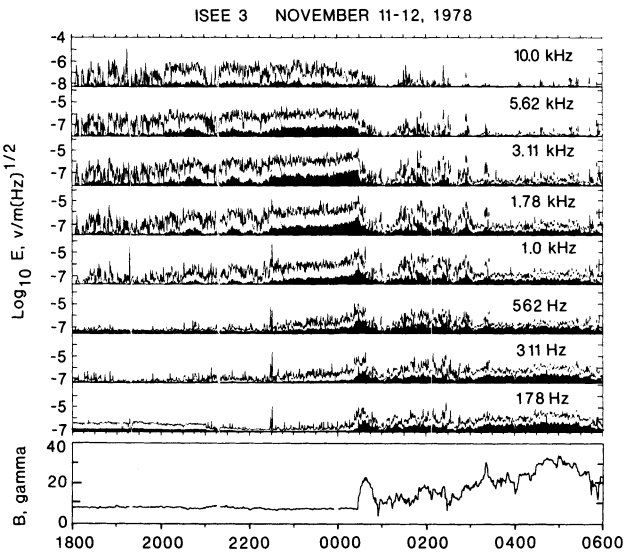

Fig. 2. Shock event of November 11–12, 1978. Twelve hours of 178 Hz–10 kHz wave electric field data surrounding the 0028 UT November 12, 1978, shock are shown together with the interplanetary magnetic field magnitude. 128-s averages are shaded, and peaks are connected by a thin line. Note the quasi-monotonic increase of the 1.0 kHz, 1.78 kHz, and 3.11 kHz amplitudes up to the shock crossing and the high peak-to-average ratio. The 178 Hz and 311-Hz electric fields are enhanced downstream, whereas the higher frequencies are suppressed downstream relative to their upstream amplitudes.

number was 4.7. In summation, the parameters of the November 12, 1978, interplanetary shock resemble those of typical quasi-parallel bow shocks.

Inspection of the interplanetary field magnitude reveals three different time periods in Figure 2. The field upstream of the shock was calm. Its magnitude jumped at the shock, increased, and then decreased to a minimum at 0054 UT. The longitude towards which the interplanetary field pointed switched from positive to negative at 0054 UT. There followed six hours of variable interplanetary field. The wave electric field data should be interpreted with these three regions in mind.

Figure 2 shows that 0.1–1 kHz and 1–10 kHz electric fields behave differently. We begin with the low frequency electric fields upstream. Interference at 178 Hz ended at 2100 UT and was absent at 311 Hz, so that the three hours prior to the shock were sampled with adequate sensitivity. The 178 and 311-Hz average amplitudes (black shading) were always at threshold upstream, whereas subsequent to 2210 UT the peak amplitudes (thin lines) measured in a 128-second cycle were slightly enhanced. At higher frequencies, 1–10 kHz, both the average and peak amplitudes were enhanced upstream. Variable activity began before 1900 UT; the average amplitudes at 1.0 kHz, 1.78 kHz, and 3.11 kHz jumped near 2230 UT. There was no local magnetic field signature associated with the jump in average amplitude at 2230 UT. Thereafter, the 1.00–3.11 kHz amplitudes increased more or less monotonically until the shock encounter at 0028 UT. These monotonic average amplitude increases suggest that the (1.00–3.11 kHz) waves were caused by the oncoming shock.

The 1.78 kHz, 3.11 kHz, and 5.62 kHz amplitudes decreased at the shock (0028 UT). A shock-associated enhancement at lower frequencies (178 Hz, 311 Hz, 562 Hz) persisted until about 0054 UT. The amplitudes at all frequencies minimized at 0054 UT. Downstream of 0054 UT, the frequencies <1.78 kHz had variable average and peak amplitudes. The 1.78- to 10-kHz noise downstream was weaker and more intermittent than that upstream.

Figure 3 shows 311 Hz and 3.11 kHz electric fields, 31 Hz magnetic fields, the interplanetary field magnitude B, and its north-south component B_Z for 30 min surrounding the shock. Every 311 Hz and 3.11 kHz electric field data point, recorded at 1/2-s intervals, is displayed. Four 31-Hz magnetic field data points 1/2 s apart are recorded consecutively for every 32 electric field points so that the fluctuating magnetic fields are sampled at intervals of 16 s.

The jump in low frequency magnetic noise at the shock is the most striking new feature in Figure 3. The 31-Hz magnetic field amplitude increased by 2 orders of magnitude in less than 16 s and remained enhanced for many hours downstream.

Figure 2 showed that the 3.11-kHz electric fields had a highly variable amplitude upstream. Figure 3 reveals that the enhanced average amplitudes, denoted by black shading in Figure 2, were made by signals that appeared impulsive on a 1/2-s time scale, whose minimum and maximum amplitudes both rose above the instrumental threshold. Their amplitudes varied by an order of magnitude from point to point.

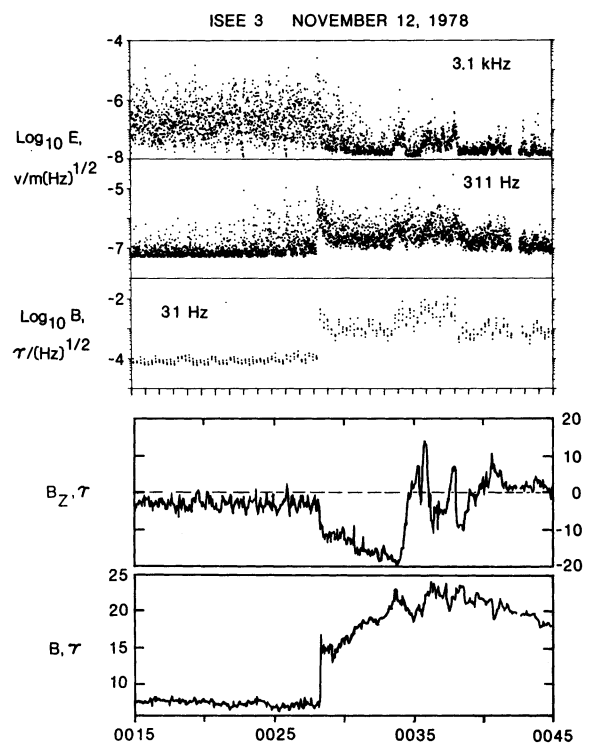

Fig. 3. High-time resolution electric and magnetic fields; November 12, 1978. Shown here are 30 min of data surrounding the November 12, 1978, shock. The data display ends just before the interplanetary field dip at 0054 UT apparent in Figure 2. The 311 Hz and 3.11 kHz electric field channels are sampled every 1/2 s, whereas the 3.1-Hz magnetic field is sampled every 16 s. Every data point is shown. The interplanetary field magnitude B and z component B_z are shown at the bottom. Note the 'stochastic' 3.11-kHz amplitude distribution upstream of the shock. Furthermore, the 31-Hz amplitude, which is near threshold upstream (see Figure 6), jumps by at least two orders of magnitude at the shock. This enhancement persists downstream.

The peak amplitudes peaked at the shock and decayed within a few minutes. Except for a few bursts, most of the data points were at the instrumental threshold thereafter. In contrast with the 3.11-kHz electric field, the 311-Hz impulsive noise upstream rose to peaks only a factor 10 above background. Most of the data points were at threshold, and 311 Hz impulses were much less frequent than those at 3.11 kHz. The 311-Hz noise peaked sharply at the shock. The average 311-Hz amplitude was an order of magnitude larger downstream than upstream, and the burst minima were all above threshold.

Figure 4 shows sample electric field spectra upstream, near, and well downstream of the shock. Since the amplitudes are variable, a succession of individual spectra compiled over 1/2 s would not be particularly revealing. Accordingly, we present the peak and minimum amplitudes obtained in each frequency channel over a 16-s cycle, together with an arbitrarily chosen single 1/2-s scan. By inspection of wave data, we can precisely locate the shock at 0028:16 UT. Since the shock speed was 700–800 km/s, the preshock spectrum beginning at 0025:36 UT was 10–15 R_E upstream of the oncoming interplanetary shock, about the distance at which events upstream of the earth's bow shock are observed. The shock spectrum spans the shock crossing to a few thousand kilometers downstream and thus contains no unaliased information about the turbulence in the shock front itself. The next post-shock spectrum, beginning at 0028:52 UT, was taken several R_E downstream, corresponding to typical magnetosheath measurements, and the last spectrum, commencing at 0041:35 UT, was taken several hundred R_E downstream of the shock.

The high-frequency spectral peak in the middle two insets of Figure 4 corresponds to the electron plasma frequency for the measured density of 12 particles/cm^3. The peak amplitude spectrum maximized between 1 kHz and 3 kHz upstream. As was noted previously, the peak-to-minimum ratio was more than 2 orders of magnitude. The amplitudes at all frequencies increased at the shock (0028:16 UT). While the 1–3 kHz spectral maximum was still present, the largest increase in amplitude, relative to upstream, occurred below 1 kHz. A few R_E downstream of the shock (0028:32 UT), the spectral peak moved from 3 kHz to 1 kHz, and the spectrum was relatively flat from 100 Hz to 1 kHz. A few hundred R_E downstream (0041:35 UT), the spectrum settled down to a $1/f$ form whose peak was below 100 Hz. The 16-s spectral minima were within a factor 2 of inflight threshold levels [*Scarf et al.*, 1981].

In summation, Figure 4 confirms the impression gained from Figure 3. The wave amplitudes were highly variable, as illustrated by the large peak-to-minimum amplitude ratios. Nonetheless, the peak spectrum had persistent features that varied consistently across the shock. The upstream spectral peak near 3 kHz disappeared at or just downstream of the shock and was replaced by one below 1 kHz. There was a progression to a lower frequency, lower amplitude spectrum with increasing distance and time downstream.

4. Shock Event of April 4–5, 1979

The interplanetary field data in Figure 5 and common data pool information reveal the potential interest of the April 4–5, 1979, shock event. The magnetic field magnitude B_T was relatively constant until the shock passed over the spacecraft at about 0120 UT. B_T jumped from 13γ to 29γ at the shock and increased thereafter to a maximum of 38γ between 0120 UT and 0720 UT. The period from 0720 UT to 0950 UT is especially interesting. B_T began an irregular decline at 0720 UT, with an especially sharp drop at 0800 UT, and reached a minimum of 10γ just before 0900 UT, whereupon it suddenly recovered to 34γ; B_T jumped again to 40γ at 0950 UT. The solar wind density increased from 12 cm^{-3} at 0720 UT to reach a broad maximum of about 90 cm^{-3} during the main magnetic field minimum between 0840 UT and 0900 UT. The

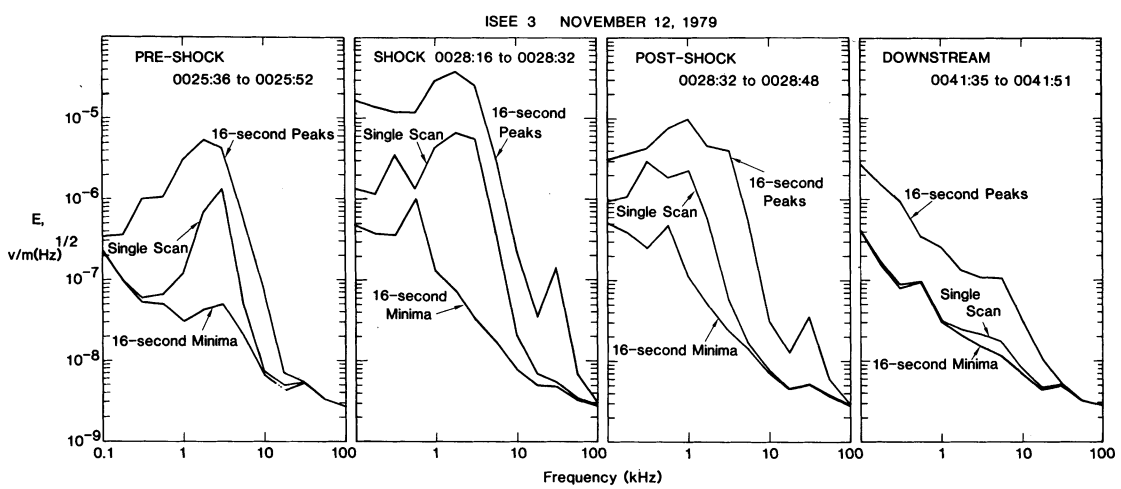

Fig. 4. Electric field spectra at points surrounding the November 12, 1978, shock. Shown here are peak and minimum electric field spectra sampled over 16-second intervals, together with an arbitrarily chosen single 1/2-s spectrum, taken 10–15 R_E upstream, at the 0028:16 UT shock, a few R_E downstream, as well downstream. The highly impulsive component, with a spectral peak near 3.11 kHz, is evident upstream. The panel labeled 'shock' includes data immediately downstream of the shock. All frequency components are enhanced, but the largest enhancement relative to upstream is at frequencies <1 kHz. The 'post-shock' spectrum, in the third panel from the left, was taken a few R_E downstream from the interplanetary shock to facilitate comparison with terrestrial magnetosheath spectra. The <1 kHz enhancement persists, and the spectral peak near 1 kHz is less pronounced. Well downstream (fourth panel) the 16-s minimum and single scan spectra are near the inflight threshold (see Figure 6), whereas the peaks are an order of magnitude larger.

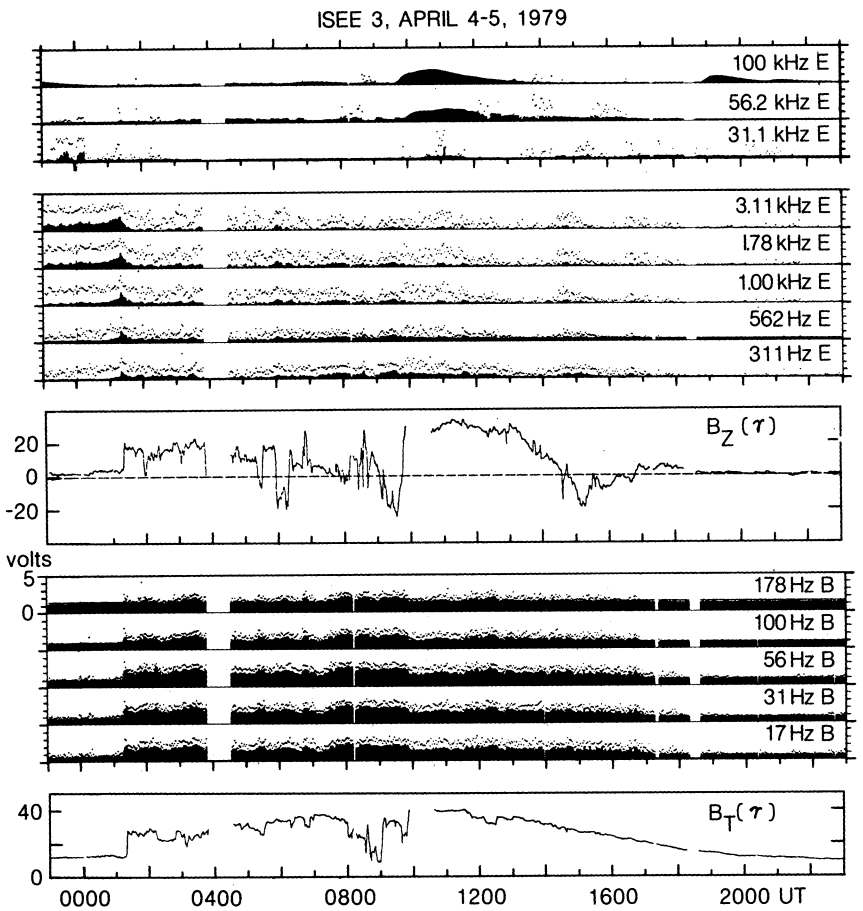

Fig. 5. Shock event of April 4–5, 1979. Shown here are 24 hours of wave electric and magnetic fields, together with the interplanetary magnitude B_T and z component B_z, for a period that includes the region upstream of the shock, apparent in the increase of 1 kHz, 1.78 kHz, and 3.11 kHz average electric field amplitudes, the shock at 0120 UT on April 25, 1979, the dense hot piston (0800–0950 UT), and the subsequent low-β ordered interplanetary field further downstream. 17- to 178-Hz magnetic and 311 Hz- to 1-kHz electric amplitudes are generally enhanced throughout the downstream region. Note the burst of 31.1 kHz electron plasma oscillations about an hour upstream of the shock and the enhancement of the 56.2 kHz continuum about an hour downstream. The 100-kHz event commencing about 0950 UT is a type III radio burst that subsequently spreads to lower frequencies.

density decreased from 90 cm^{-3} to 50 cm^{-3} at the B_T increase at 0900 UT and decreased again from 50 cm^{-3} to 5 cm^{-3} at the second B_T jump at 0950 UT. The solar wind speed increased from slightly below 600 km/s at 0720 UT to slightly above 700 km/s at 0900 UT. The high densities and low magnetic field strengths suggest that β was large between 0800 UT and 0950 UT. Moreover, the simultaneous decreases in density and increases in magnetic field suggest that approximate pressure equilibrium was maintained across the interfaces at 0900 UT and 0950 UT. If so, the sum of the electron and ion temperatures was about 60 eV ahead of each interface, and β was about 20 ahead of the 0900 UT interface. The period between 0800–0950 UT may thus be associated with the passage of a dense, hot plasma over ISEE 3. The period after 0950 UT differed considerably from the one preceding it. After the magnetic field increase and strong rotation at 0950 UT, B_T decreased smoothly and almost monotonically to the preshock value at 2000 UT. Since the solar wind density was relatively low throughout this period, we surmise that β was also low.

The wave electric fields associated with the April 4–5, 1979, and November 11–12, 1978, shock events are similar. The average and peak amplitudes of the upstream 1- to 10-kHz electric fields began to be enhanced above threshold at 1300 UT on April 4, 1979. A persistent quasi-monotonic increase began at about 2000 UT. Following a one-hour data gap ending at 2300 UT, the persistent increase continued until the shock encounter at 0120 UT on April 5, 1979. This last portion of data is shown in Figure 5 for the 1.00 kHz, 1.78 kHz, and 3.11 kHz channels. Note the high peak-to-average ratios throughout, the sharp intensity spike of about 10-min duration at the shock, and the suppression of the peak and, especially, average amplitudes downstream—all features encountered in the November 11–12, 1978, shock event. Amplitude plots on the same time scale as that of Figure 3 reveal a similar 'stochastic' amplitude distribution for the upstream 1- to 10-kHz electric field noise.

The low-frequency (0.1–1 kHz) electric fields had a persistent small increase in peak amplitudes for two hours prior to the shock. The average 311 Hz and 562-Hz amplitudes were below threshold at this time. The peaks and averages maximized at the shock and decayed downstream in about ten minutes. Thereafter, the peaks and averages remained generally above their upstream values, with the exception of the period 0340–0600 UT, until the second interface at 0950 UT. The average 311-Hz amplitude was especially enhanced in

the high β region between 0720 UT and 0950 UT. After 0950, the peak and average amplitudes decreased, though not monotonically.

The peak and average low-frequency magnetic field fluctuations (17.8–178 Hz), which were generally below threshold upstream, were strongly enhanced at the shock. The 17.8-100 Hz peaks and averages both rose above threshold, and the 178 Hz peaks exceeded threshold at the shock. The downstream amplitudes were comparable with those found on November 11–12, 1978. The amplitude enhancement persisted from the shock at 0120 UT to the second interface at 0950 UT. The amplitudes were not monotonic between the shock and second interface, making it difficult to argue that the waves were generated at the shock and decayed slowly downstream. They were enhanced in the high β region between 0720 UT and 0950 UT and remained virtually constant throughout this period, despite the large changes in plasma β that took place. Their amplitudes dropped by an order of magnitude at 0950 UT and decreased slowly thereafter. The 178-Hz peaks sank below threshold at 1600 UT, and all channels were below threshold at 1800 UT, when the interplanetary field re-achieved a quiet state.

An association between low-frequency magnetic field fluctuations and a disordered interplanetary magnetic field is apparent in Figure 5. Between the shock and the second interface (0120–0950 UT), the interplanetary field direction was highly disordered, an effect particularly noticeable in B_Z; during this period, low frequency magnetic fluctuations were enhanced. After the data gap ending about 1030 UT, B_T began its many-hour-long decrease, and both the variability of the interplanetary field and the low-frequency magnetic amplitudes decreased. By 1800 UT, all components of the interplanetary field became steady, and the low-frequency magnetic amplitudes dropped below threshold.

The top panel of Figure 5 shows 31.1 kHz, 56.2 kHz, and 100 kHz electric field data for the shock event of April 4–5, 1979. Several impulsive bursts, which also enhanced the average amplitudes at 31.1 kHz, occurred between 2330 UT on April 4, 1979, and 0015 UT on April 5, 1979, about an hour upstream of the shock. During this period the ion density ranged between 3.0 and 9.3 cm^{-3}, so that the electron plasma frequency was 25.5–27.4 kHz, below but near the center frequency of the 31.1-kHz channel. Thus these bursts were electron plasma waves. The electron plasma frequency jumped to 49 kHz at the shock, which was marked by a few short bursts in the neighboring 31.1 kHz and 56.2-kHz channels. Besides bursts, the 56.2 kHz and 100-kHz channels recorded enhanced nonimpulsive noise throughout the event. The 56.2-kHz steady component intensified about an hour downstream of the shock. This intensification spread to the 100-kHz channel during the broad density increase between 0840 UT and 1000 UT, during which time the electron plasma frequency ranged between 64 kHz and 85 kHz. A type III radio burst, identifiable by its characteristic time profile, commenced at 100 kHz at about 0940 UT, spread subsequently to 56.2 kHz and possibly to 31.1 kHz, and remained detectable until 1700 UT at 56.2 kHz. The onset of the burst roughly coincided with a diminution of the 17.8–178 Hz magnetic fluctuations.

5. Forward and Reverse Shock Pair, April 24–25, 1979

An incomplete data sample prevents a complete study of the entire region between the forward shock encountered at 2327 UT on April 24, 1979, and the reverse shock at 1250 UT on April 25, 1979. However, the data do permit us to address two interesting questions. Figure 1 reveals that the April 24, 1979, forward shock had a precursor of low-frequency magnetic noise extending about 20-min upstream of the shock, which we can compare with the noise downstream. Second, we can investigate the extent to which 'upstream' phenomena were resumed downstream of the reverse shock on April 25, 1979.

Figure 6 shows the peak electric and magnetic field

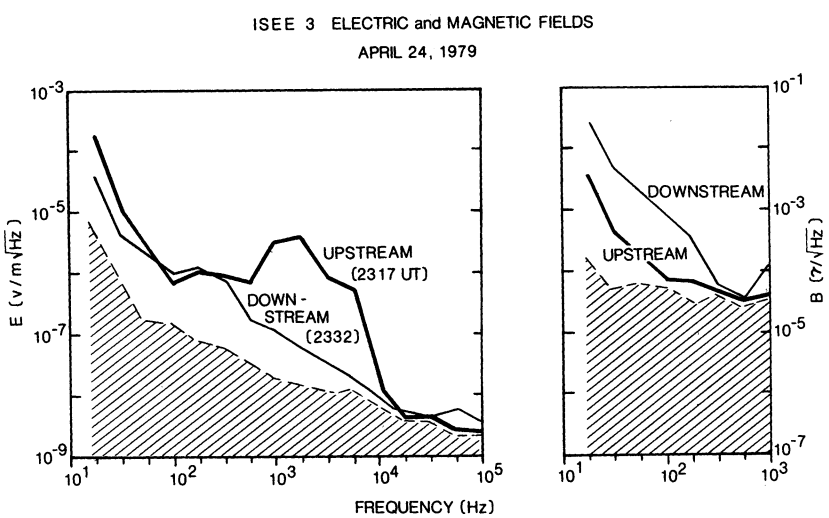

Fig. 6. Electric and magnetic spectra upstream and downstream of the April 24, 1979, forward shock. The left inset shows the 17 Hz–100 kHz electric field spectra, and the right inset shows the 17 Hz–1 kHz magnetic spectra obtained upstream (heavy line) and downstream (light line) of the April 24, 1979, shock. Shown are peak amplitudes recorded over a 1-minute interval. Amplitudes below the inflight calibrated threshold are shaded. The upstream and downstream E field spectra are similar to those in Figure 5. The upstream magnetic spectrum was taken in the 'foot' noted in Figure 1. The waves are above threshold only below 100 Hz, whereas downstream the spectrum extends out to 300 Hz. The upstream waves may have a steeper spectrum than those downstream.

amplitudes recorded over 1-min intervals beginning at 2317.01 UT, about 9 min upstream of the April 24, 1979, forward shock, and at 2332.09 UT, about five minutes downstream. Amplitudes below the inflight calibrated threshold [*Scarf et al.*, 1981] are shaded. The left hand inset of Figure 6 shows electric field peak amplitudes. Impulsive broadband noise, peaking at 3.16 kHz, was again encountered upstream of the April 24, 1979, forward shock. Down-

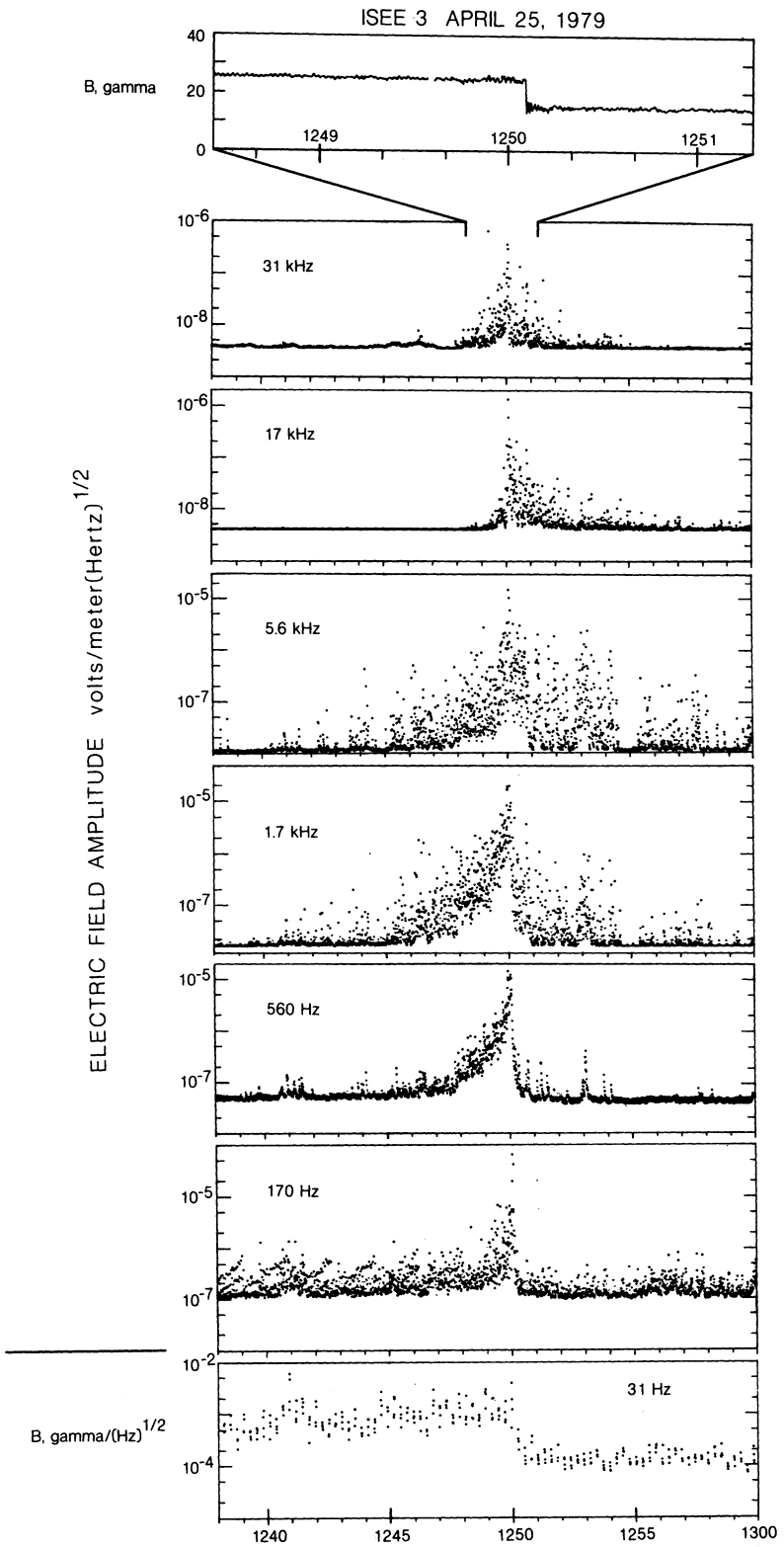

Fig. 7. Reverse shock of April 25, 1979. Shown here are three minutes of interplanetary field magnitude data, and 22 min of wave electric and magnetic field data surrounding the 1250 UT passage of a reverse shock on April 25, 1979. Note that impulsive 5.6 kHz electric field noise, which builds up before the shock, persists downstream (see also Figure 1). The low frequency 31-Hz magnetic noise drops by an order of magnitude at the shock to about threshold downstream.

stream, the electric field spectrum was dominated by low-frequency noise with a small spectral peak near 178 Hz and 316 Hz. The peak-to-average amplitude ratio was about 5 at 316 Hz downstream, whereas it was about 10 at 3.16 kHz upstream. The right-hand inset of Figure 6 shows magnetic field peak amplitudes. The 1-min average amplitudes were no more than a factor of 3 lower than the peaks over the entire 17.8 Hz–1 kHz frequency range both upstream and downstream. The downstream peak magnetic amplitudes were a factor 10–20 larger than the upstream amplitudes. The spectrum of the upstream precursor was steeper than that downstream at the lowest frequencies.

Figure 7 shows 3-min of interplanetary magnetic field data and 22 min of wave electric and magnetic field data surrounding the reverse shock passage at 1250:05 UT on April 25, 1979. The sudden decrease of the magnetic field from 25γ to 15.7γ identifies this event as a discontinuity. The decrease in ion density from 18.5 cm^{-3} to 4.5 cm^{-3} suggests it was a reverse shock in the fast MHD mode. The electron plasma frequency was about 38 kHz upstream and 18 kHz downstream. The 17.8 kHz and 31.1-kHz electric field channels nearest these plasma frequencies were active for about 5-min surrounding the reverse shock passage, with strong amplitude peaks at the shock. The 5.6-kHz electric field noise, which built up several minutes before the reverse shock, returned to the impulsive behavior typically found upstream of forward shocks. Impulsive behavior persisted in the 1.78 kHz, 3.16 kHz, and 5.62 kHz channels until the end of the day. The 31.1 Hz magnetic amplitudes decreased from an amplitude of about $10^{-3}\gamma/\sqrt{Hz}$ upstream of the shock to about $10^{-4}\gamma\sqrt{Hz}$ downstream, about a factor of 2 above the inflight threshold. In summation, low frequency magnetic turbulence was confined upstream of, and impulsive 1- to 10-kHz electric field noise resumed downstream of, the April 25, 1979, reverse shock.

6. SHOCK EVENTS OF JUNE 6–7, 1979, AND NOVEMBER 29–30, 1979

In this section we discuss two high density shocks that had quasi-steady electron plasma waves many hours upstream of them.

Figure 8 shows 24 hours of wave electric and magnetic fields, together with the interplanetary field magnitude B_T, for the shock event of June 6–7, 1979. We begin by describing the interplanetary field magnitude profile. A period of calm B_T was replaced at 0800 UT on June 6–7, 1979, by one of greater disturbance that continued until the shock encounter at 1845 UT, where the magnetic field jumped from 13γ to

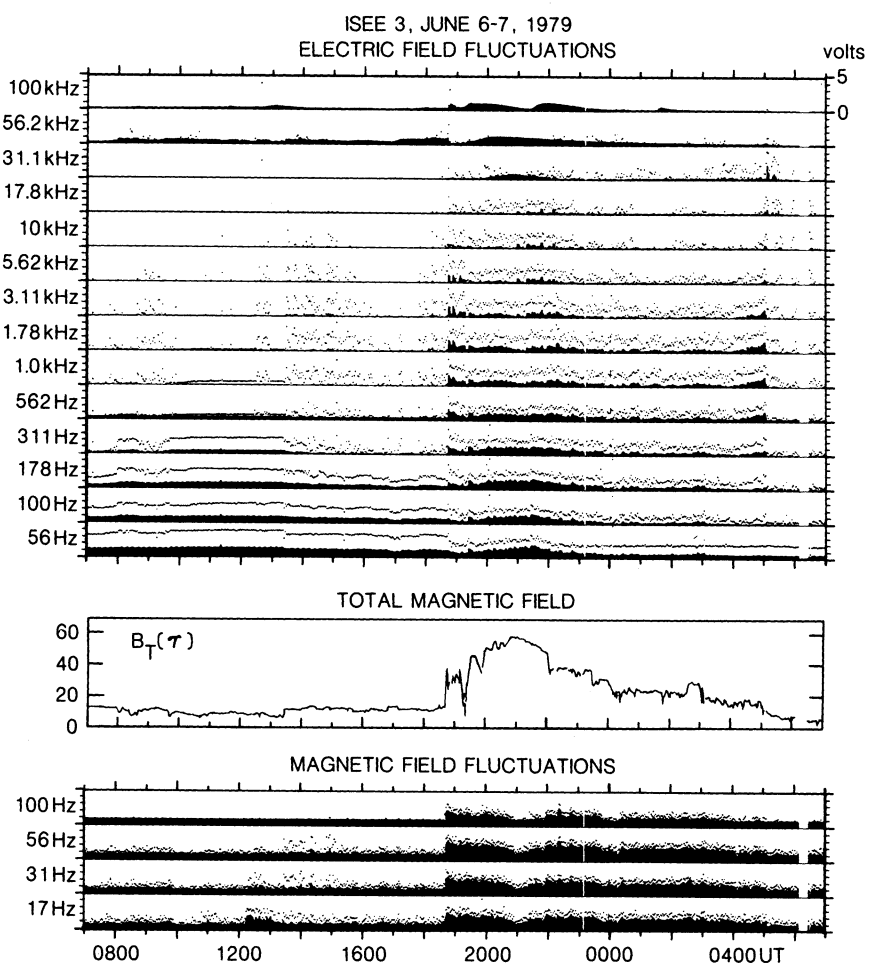

Fig. 8. Shock event of June 6–7, 1979. Shown here are 24 hours of wave electric and magnetic field together with interplanetary field magnitude data surrounding the shock of June 6, 1979, which is apparent by the increase in low-frequency magnetic fluctuations. There is a possible developing reverse shock near 0500 UT on June 7, 1979. The impulsive 1 kHz–10 kHz electric field component was largely absent upstream, and the 100 Hz–1.78 kHz component was generally enhanced throughout the disturbed region. The 56.1-kHz continuum was enhanced near 0800 UT and jumped to 100 kHz at the shock, consistent with the measured density increase.

27γ. The solar wind density, which was unusually large (27 cm^{-3}) upstream, jumped to 112 cm^{-3} downstream. B_T remained near 30γ after the shock until it suddenly dipped to 10γ at 1920 UT. It then recovered and began a gradual increase to a maximum of 55γ at 2100 UT. This period of strong magnetic field terminated in a decrease at 2145 UT, followed by a gradual but structured decline that brought B_T back to its undisturbed state through a final small sudden decline near 0500 UT on June 7, 1979.

The magnetic field profile in Figure 8 suggests that the June 6, 1979, shock had a different driver than did that of April 5, 1979. Common data pool information confirms this impression: The solar wind density, which increased from 27 cm^{-3} to 112 cm^{-3} at the shock, dropped back to 75 cm^{-3} ten minutes downstream. Accompanying the magnetic field dip at 1920 UT was a sharp decline in density, from 78 cm^{-3} to 25 cm^{-3}. Thereafter, while the magnetic field recovered and increased, the density commenced a further slower decline, reaching extremely low values (1–2 cm^{-3}) between 2115 UT and 2145 UT. The solar wind speed increased from 450 km/s at 1930 UT to above 900 km/s just before the interface at 2145 UT. On crossing the interface, B_T decreased, the density returned to 25–30 cm^{-3}, and the solar wind speed diminished to 550 km/s. Thus the driver of the June 6, 1979, shock was a low density fast stream that may have been terminated by a developing reverse shock near 0500 UT on June 7, 1979.

Upstream electric field activity at frequencies exceeding 10 kHz is the new feature of the wave data. The transition to a more variable B_T at 0800 UT on June 6, 1979, was accompanied by a rotation of the magnetic field direction (not shown) and a sharp enhancement of the steady 56.2 kHz electric fields that persisted until the shock encounter. 56-kHz corresponds to the plasma frequency for an electron density of 25 cm^{-3}, consistent with the measured ion density. The steady 56-kHz noise was therefore due to electron plasma waves. The brief burst of 100 kHz plasma wave noise initiated at the shock is consistent with the density compression to over 100 cm^{-3} that lasted about 10 min downstream. This burst disappeared and was replaced by a type III radio burst after 1900 UT. The type III burst spread first to 56.2 kHz and to 31 kHz between 2000 UT and 2200 UT, during most of which time the solar wind density was less than 15 cm^{-3}. Since type III bursts are radiated at or above the electron plasma frequency, their appearance at 31.1 kHz is consistent with the low ion densities measured during this time. The low densities (1–2 cm^{-3}) measured between 2115–2145 UT suggest that the bursts of 10 kHz and 17.8-kHz noise in this interval may also have been electron plasma waves.

Let us now turn to the 0.1- to 10-kHz electric fields. There were virtually no waves upstream except for a few impulsive bursts. The wave phenomena between 311 Hz and 10 kHz at and immediately downstream of the shock were similar to those in other shocks. The shock enhancement was largest at frequencies at and below 1.78 kHz, and the behavior at higher frequencies was similar to that found downstream elsewhere. The fast stream encounter, between the magnetic field dip at 1920 UT and the interface at 2200 UT, must be treated with caution, especially the period of lowest density (2115–2145 UT), when every electric field channel up to, and perhaps above, the electron plasma frequency was active. There was no gap separating the 'ion acoustic' and 'electron plasma wave' frequency ranges.

Following the interface at 1100 UT, activity above 1.78 kHz disappeared except for sporadic bursts. However, the intermediate frequency channels (311 Hz–1.78 kHz) remained enhanced and active until the final magnetic field dip at 0500 UT on June 7, 1979, which we tentatively identified as a developing reverse shock. The average amplitudes built up monotonically for an hour before this event. There was a burst of 31.1-kHz waves at the event, which may have been electron plasma waves. Thereafter, the activity level returned to one similar to that encountered upstream of the shock, except that electron plasma waves were absent.

Unlike most previous events studied, the 17 Hz, 31 Hz, and 56 Hz magnetic field channels were active many hours upstream of the shock, though the peaks upstream, at most, equalled the average amplitude downstream. A particularly interesting burst between 1210 UT and1305 UT was concentrated in the 17-Hz channel (or below). Its frequency spectrum therefore differed from the broader-band spectrum downstream of the shock. As in other shocks, the low-frequency (17–100 Hz) magnetic amplitudes increased by two orders of magnitude at the shock and decreased quasi-monotonically downstream, with the exception of the dip near 2100 UT interface. The activity diminished to its upstream level after the possible developing reverse shock at 0500 UT on June 7, 1979.

The events of November 29 and 30, 1979, shown in Figure 9, are unusual because the most significant wave electric field activity during the entire 24-hour period took place at 56.2 kHz and 100 kHz. Impulsive 1- to 10-kHz electric field activity, similar to that found upstream of other shocks, commenced at about 0700 UT on November 29, 1979 (not shown), and continued until it terminated in a weak shock at 1539 UT on November 29, 1979. The magnetic field and ion number density jumped from 2.9γ to 4.8γ and 18.7 cm^{-3} to 35.8 cm^{-3} at the 1539 UT shock. Low amplitude 17.8–56.2 Hz magnetic oscillations began at the shock and persisted until a second shock crossing at 0650 UT on November 30, 1979. Virtually the only electric field activity between the two shocks was at 56.2 kHz, near the 54 kHz electron plasma frequency based on the ion density measured near 1539 UT. The electron plasma wave amplitudes varied smoothly between the shocks, and occasional impulsive bursts began about an hour upstream of the 0650 UT shock. At this shock, the ion density increased from 33 cm^{-3} to 99 cm^{-3}, and the electron plasma wave activity shifted to the 100-kHz channel, reflecting the increase in density. The ion density remained above 80 cm^{-3} until about 730 UT. The magnetic field jumped from 13γ to 37γ at 0650 UT. The shock was followed by a field magnitude dip about 45 minutes later. The enhanced electric field activity shifted from 100 kHz to 56.2 kHz near the second magnetic field maximum at 0750 UT and remained in the channel, with variable average amplitude, until it terminated at the weak magnetic field decrease at 1320 UT. About two hours later (not shown), the 56.2-kHz channel was reactivated by a type III radio burst that first appeared at 100 kHz.

The ISEE 3 radio astronomy instrument, which has excellent frequency resolution between 30 kHz and 100 kHz, has detected broadband continuum enhancements at and downstream of interplanetary shocks [*Hoang et al.*, 1980]. This

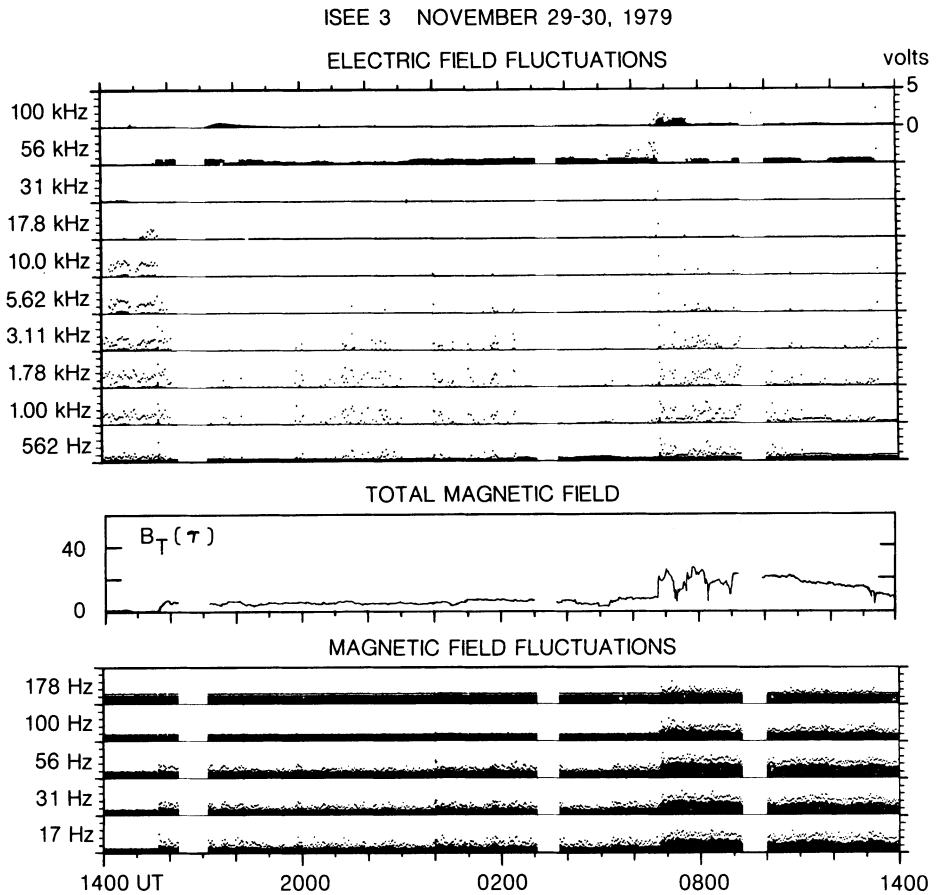

Fig. 9. Shock events of November 29–30, 1979. A weak shock at 1539 UT on November 29, 1979, preceded a stronger one at 0650 UT. The 56.2 kHz continuum and the low-frequency magnetic fields were enhanced at the 1539 UT shock and persisted until the 0650 UT shock, where the continuum jumped to 100 kHz, with some impulsive bursts, and the low-frequency magnetic fields jumped again. Impulsive 1 kHz–10 kHz electric field noise was present only upstream of the 1539 UT shock, and the lower frequency electric field component was largely absent, except for a few bursts, downstream of either shock.

continuum has a low-frequency cutoff at the electron plasma frequency, a peak of variable intensity above the plasma frequency, and a smaller peak at twice the electron plasma frequency. The steady noise near the electron plasma frequency detected by the ISEE 3 plasma wave instrument is similar to the continuum studied by *Grigorieva and Slysh* [1970], *Brown* [1973], *Gurnett* [1975], *Weber et al.* [1976], and *Hoang et al.* [1980]. Though our electron plasma wave measurements have inadequate frequency coverage, they are consistent with those reported by *Hoang et al.* [1980]. An enhancement of the steady plasma wave noise occurs for each of the shocks presented in this paper, including the August 26–27, 1978, event studied both by us and *Hoang et al.* [1980]. *Grigorieva and Slysh* [1970], *Meyer-Vernet* [1979], and *Hoang et al.* [1980] interpret the continuum as due to thermal plasma wave fluctuations. If so, its enhancements may be a signature of increased electron energy density.

As with other shocks, the broadband (17.8–178 Hz) magnetic field amplitudes increased at the 0650 UT shock and remained enhanced downstream, gradually dying away after 2400 UT on November 30, 1979. Impulsive intermediate frequency (561 Hz–1.78 kHz) electric fields were occasionally detected downstream of both the 1539 UT and 0650 UT shocks, though unlike other cases, their average amplitudes did not rise above threshold.

7. Comparisons of Interplanetary Shocks With the Bow Shock

While no one interplanetary shock contained all possible upstream features, ISEE 3 has detected at least once each type of plasma wave upstream of interplanetary shocks that has been reported upstream of the bow shock; these are impulsive electron plasma waves, impulsive 1- to 10-kHz electric fields, and low-frequency magnetic oscillations below the electron gyrofrequency. Thus the ensembles of plasma wave phenomena upstream of interplanetary shocks and the bow shock are similar.

Figure 10 organizes the upstream 1- to 10-kHz electric field noise by local shock normal angle. Four and one-half hours of 3.11-kHz data upstream, and one and one-half hours downstream, are shown for six shocks whose θ_{Bn} values range from 88° to 22°. The 3.11-kHz electric fields are more intense upstream from the four quasi-parallel shocks ($\theta_{Bn} \leq 51°$) than upstream from the two quasi-perpendicular shocks (θ_{Bn} = 88°, 74°). The 3.11-kHz noise intensifies downstream of the quasi-perpendicular shocks. 1- to 10-kHz waves were also found hours upstream of a quasi-parallel shock (θ_{Bn} = 15°) observed by Voyager 1 [*Burlaga et al.*, 1980]. The conclusion drawn from Figure 10, that only quasi-parallel shocks have upstream noise in the several kiloHertz

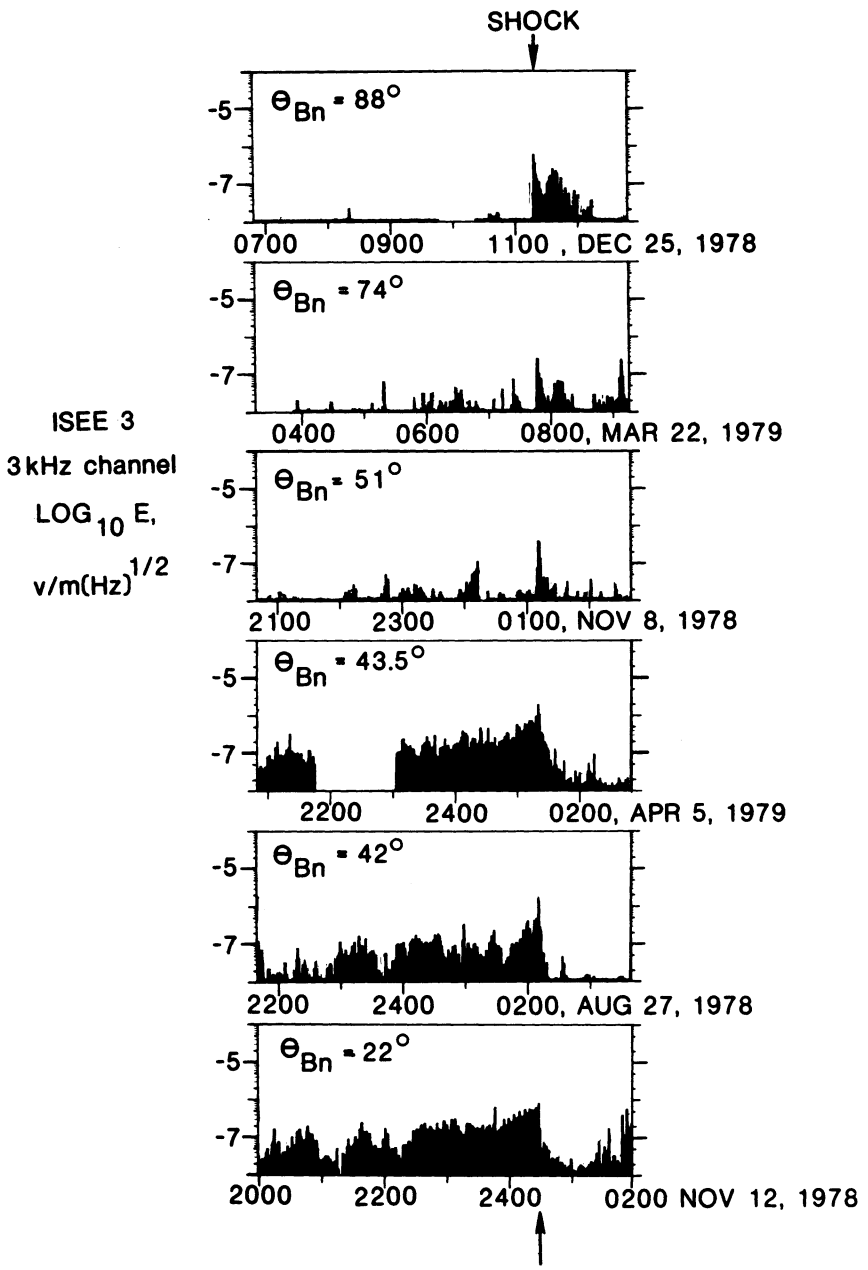

Fig. 10. 3.16 kHz electric field noise organized by θ_{Bn}. Shown here are 4.5 hours of 3.16-kHz electric field data upstream and 1.5 hours downstream of 6 interplanetary shocks ordered by local shock normal angle θ_{Bn}. θ_{Bn} ranges from 22° to 88°. The quasi-parallel shocks ($\theta_{Bn} < 51°$) in this display have impulsive 3.16-kHz noise upstream, whereas it appears downstream of the quasi-perpendicular shocks.

range, must be regarded as tentative. We have yet to compute the detailed time-dependent connection of the upstream magnetic fields to the shocks. Such computations may help us understand the exceptions to the rule implied by Figure 10; e.g., why the April 24, 1979, shock was quasi-perpendicular when it passed over ISEE 3, yet had variable upstream 1-10 kHz noise, or why the locally quasi-parallel June 6, 1979, shock had little noise upstream.

Figure 11 compares electric field spectra upstream from the six interplanetary shocks in Figure 10 with an ISEE 2 bow shock spectrum [*Anderson et al.*, 1981]. The ISEE 3 peak spectra compiled over the 16-s data frame preceding the one containing the shock are shown. These spectra were therefore compiled about 20 s, or about 1–2 R_E, upstream of the shocks. We have distinguished between the quasi-parallel ($\theta_{Bn} < 51°$) and quasi-perpendicular shocks by using solid (Q ∥) and dotted (Q ⊥) lines. The quasi-parallel spectra are similar to one another and contain a factor of 10^6 more power between 1–10 kHz than the quasi-perpendicular shocks. The ISEE 2 peak spectrum was also taken about an earth radius upstream of the bow shock. Its shape is similar to the interplanetary quasi-parallel spectra, but its overall amplitude level is larger. However, *Anderson et al.* [1981] have shown that the 1- to 10-kHz noise appears more intense using the ISEE 2 30-m antenna than using the ISEE 1 215-m antenna. They infer that the 1- to 10-kHz wavelengths are

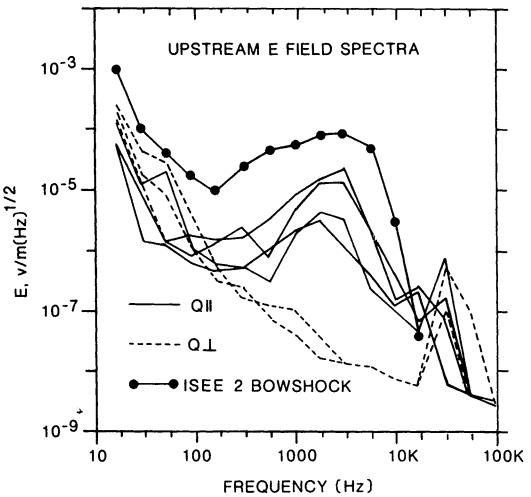

Fig. 11. Comparison of upstream interplanetary and bow shock electric field spectra. The peak spectra about 1–2 R_E upstream of the six interplanetary shocks in Figure 10 are compared with an ISEE 2 peak spectrum [*Anderson et al.*, 1981] recorded a comparable distance upstream of the bow shock. The quasi-parallel interplanetary shocks ($\theta_{Bn} < 51°$, solid lines) have much more power than the quasi-perpendicular (dotted lines) shocks, as suggested by Figure 10. In addition, the quasi-parallel ISEE 3 spectra are similar in shape to the ISEE 2 spectrum. We expect that the ISEE 2 signal strength would have been weaker had it been detected with ISEE 3's 90-m antenna. The inflight calibrated ISEE 3 electric field threshold is plotted in Figure 6.

between 30 and 215 m. The ISEE 3 90-m antenna would have recorded a weaker signal than the ISEE 2 spectrum in Figure 11.

Because the peak 1- to 10-kHz electric field spectra ~1 R_E upstream of quasi-parallel interplanetary shocks and the bow shock are similar, more detailed aspects of bow shock observations may apply to interplanetary shocks. 1- to 10-kHz electric field noise ahead of the bow shock is longitudinal and polarized parallel to the instantaneous interplanetary field [*Gurnett and Frank*, 1978; *Anderson et al.*, 1981]. Its wavelength [*Anderson et al.*, 1981] and spectrum are consistent with Doppler-shifted ion acoustic waves [*Gurnett and Frank*, 1978; *Kellogg*, 1981]. Because the solar wind is supersonic and super-Alfvénic, ion acoustic, as well as Alfvén and fast MHD, waves will be blown downstream, perhaps into the shock. Shock-associated ion acoustic waves must, therefore, be generated by fast particles escaping upstream. Indeed, the ISEE 2 ion waves in Figure 11 occurred after the interplanetary field rotated to connect the spacecraft to the shock, and the few keV ion fluxes increased by a factor of 100 [*Anderson et al.*, 1981]. These ion fluxes fluctuated violently, perhaps because of spatial gradients convecting over the spacecraft [*Parks et al.*, 1981]; LEPEDEA measurements, compiled over 2 min, revealed the ion distribution to be 'diffuse.' Since diffuse ions are associated with upstream ULF waves [*Paschmann et al.*, 1979], it is no surprise that diffuse ions, ion acoustic waves, and ULF waves occurred simultaneously [*Anderson et al.*, 1981; *Parks et al.*, 1981) on field lines that probably connected to the quasi-parallel shock zone. Our ISEE 3 observations suggest that not only may ion acoustic waves and perhaps other related phenomena occur far upstream of quasi-parallel interplanetary shocks, but also comparable distances upstream from the bow shock, beyond ISEE 3. However, the observations of backstreaming energetic bow shock ions at ISEE 1 and their absence at ISEE 3 suggest that they propagate free of back-scattering beyond ISEE 3 [*Scholer et al.*, 1980]. This may mean that strong MHD turbulence may not extend as far upstream as ion acoustic turbulence.

Figure 12 compares ISEE 3 peak electric field spectra from the first complete 16-s frame following the shock with an IMP 6 magnetosheath spectrum [*Rodriquez*, 1979]. All spectra were taken a few R_E downstream of the shocks. The quasi-parallel and quasi-perpendicular interplanetary spectra are similar to one another. Moreover, the interplanetary and magnetosheath spectra have comparable amplitudes, although the flat portions of the interplanetary spectra extend to higher frequencies than for the magnetosheath spectrum. The amplitudes of the low-frequency electric field noise downstream are similar on ISEE 1 and 2; this indicates that the wavelength exceeds 215 m [*Anderson et al.*, 1981]. To our knowledge, this mode has not been identified theoretically.

Figure 13 compares low-frequency peak magnetic spectra taken in the 16-s data frames immediately preceding and following the six shocks in Figure 10. The peak and average amplitudes are similar. The wave amplitudes are about a factor of one hundred smaller upstream than downstream. The downstream quasi-parallel spectra are similar to one another, and the downstream quasi-perpendicular spectra may peak near 56 Hz. *Scarf et al.* [1974], using IMP 7 data, and *Neubauer et al.* [1977], using Helios 2 data, also report enhancements of low frequency magnetic noise near interplanetary shocks. The interplanetary shock spectra published by *Gurnett et al.* [1978] and *Neubauer et al.* [1977] are similar in amplitude level and spectral shape to the downstream spectra in Figure 13. The OGO 3 magnetosheath spectrum [*Olson et al.*, 1969] is again similar to the downstream interplanetary spectra. A high Mach number labora-

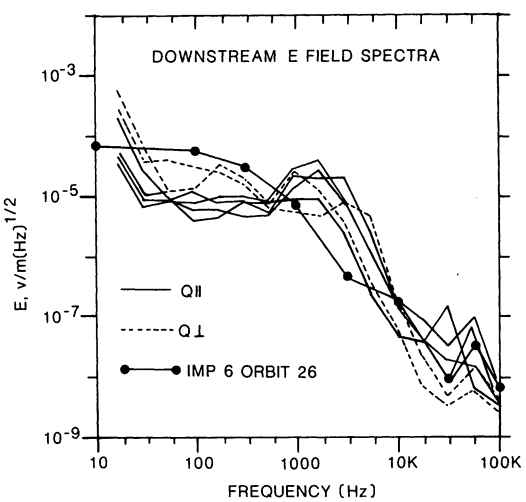

Fig. 12. Comparison of downstream interplanetary and bow shock electric field spectra. The peak electric field spectra about 1–2 R_E downstream of the 6 interplanetary shocks in Figure 10 are compared with an IMP 6 magnetosheath spectrum [*Rodriguez*, 1979]. The quasi-parallel and quasi-perpendicular interplanetary spectra are similar to one another, and to the interplanetary spectra. The power is more or less evenly distributed between 100 Hz and about 1 kHz in a mode which has not been identified conclusively.

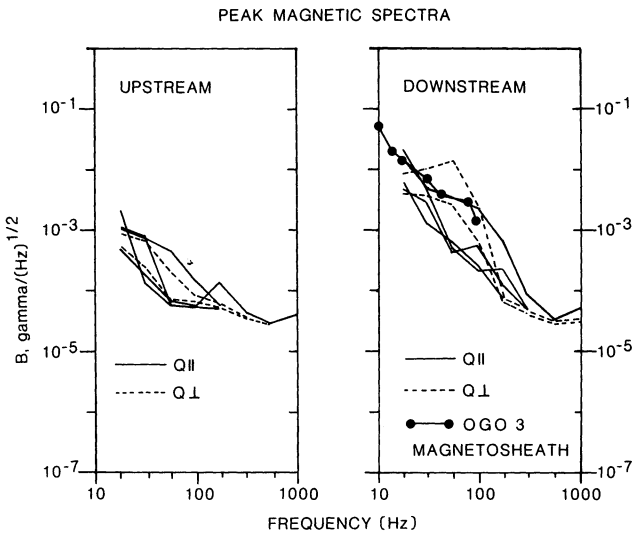

Fig. 13. Broadband low frequency magnetic noise upstream. There is little magnetic noise upstream of all six interplanetary shocks in Figure 10. The power is enhanced by a factor of 100 downstream of both quasi-parallel and quasi-perpendicular shocks, and the downstream spectra are similar to OGO 3 magnetosheath spectra [*Olson et al.*, 1969]. *Coroniti et al.* [1982] will argue that the broadband magnetic noise downstream is in the whistler mode.

tory experiment [*Podgorny*, 1979] has found magnetic turbulence downstream whose spectrum in units scaled to the ion cyclotron frequency is similar to the *Olson et al.* [1969] spectrum. A companion study [*Coroniti et al.*, 1982] will show that the low-frequency magnetic noise is in the whistler mode, as *Neubauer et al.* [1977] and *Gurnett et al.* [1978] suggested. It appears that broadband whistler noise is a ubiquitous, if not universal, feature of flowing plasmas made turbulent by shocks.

8. SUMMARY

1. The ISEE 3 plasma wave instrument detects 1–10 kHz Doppler-shifted ion acoustic bursts hours upstream from quasi-parallel interplanetary shocks. The ion acoustic spectra 1–2 R_E upstream of interplanetary shocks and the bow shock are similar in shape and intensity.

2. A lower frequency electric field component (<1 kHz) is enhanced at interplanetary shocks, and it often persists hours downstream. Its spectrum is similar to that of magnetosheath electric field noise. This component is rarely detectable upstream.

3. Broadband whistler noise increases at, and persists hours downstream from, every interplanetary shock in our sample. Its spectrum is similar to that found in the terrestrial magnetosheath. A foot of lower amplitude noise has also been found upstream from two shocks.

4. A smooth high frequency continuum near and above the local electron plasma frequency is enhanced at every interplanetary shock in our sample. This component persists for hours downstream. On two occasions, this continuum was also enhanced upstream, once by a weak shock that preceded the main one under study. Intense impulsive electron plasma waves were found about an hour upstream of one shock. Impulsive electron plasma waves are detectable for a few minutes on either side of other interplanetary shocks.

This analysis suggests that the plasma physics studied in detail near the earth's bow shock may apply to interplanetary shocks on a far larger spatial scale, a scale of interest to cosmic ray acceleration theories. The very different behavior of quasi-parallel and quasi-perpendicular shocks revealed in bow shock studies also appears in interplanetary shocks, suggesting that the observed quasi-parallel bow shock structure is intrinsic rather than accidental. If so, it would be interesting to search for MHD waves upstream of interplanetary shocks.

Acknowledgments. We would like to acknowledge useful discussion with J. T. Gosling, E. W. Greenstadt, B. T. Tsurutani, and K. P. Wenzel. This research at TRW was supported by NASA under contract NAS5-20682, and the research at the University of Iowa was supported under contract NAS5-20093 and grant NGL-16-001-043. The work at JPL represents one aspect of research carried out by JPL for NASA under contract NAS7-100.

The Editor thanks P. J. Kellogg and S. P. Gary for their assistance in evaluating this paper.

REFERENCES

Abraham-Shrauner, B., and S. H. Yun, Interplanetary shocks seen by Ames plasma probe on Pioneer 6 and 7, *J. Geophys. Res., 81,* 2097, 1976.

Anderson, K. A., Energetic electrons of terrestrial origin upstream in the solar wind, *J. Geophys. Res., 73,* 2387, 1968.

Anderson, K. A., Energetic electrons of terrestrial origin behind the bow shock and upstream in the solar wind, *J. Geophys. Res., 74,* 95, 1969.

Anderson, K. A., R. P. Lin, F. Martel, C. S. Lin, G. K. Parks, and H. Reme, Thin sheets of energetic electrons upstream from the earth's bow shock, *Geophys. Res. Lett., 6,* 401, 1979.

Anderson, R. R., G. K. Parks, T. E. Eastman, D. A. Gurnett, and L. A. Frank, Plasma waves associated with energetic particles streaming into the solar wind from the earth's bow shock, *J. Geophys. Res., 86,* 4493, 1981.

Axford, W. I., E. Leer, and G. Skadron, The acceleration of cosmic rays by shock waves, *Proc. Int. Conf. Cosmic Rays, 15th, 11,* 132, 1977.

Bame, S. J., J. R. Asbridge, W. C. Feldman, J. T. Gosling, G. Paschmann, and N. Sckopke, Deceleration of the solar wind upstream from the earth's bow shock and the origin of diffuse upstream ions, *J. Geophys. Res., 85,* 2981, 1980.

Bame, S. J., J. R. Asbridge, W. C. Feldman, J. D. Gosling, and R. D. Zwickl, Bi-directional streaming of solar wind electrons > 80 eV: ISEE evidence for a closed-field structure within the driver gas of an interplanetary shock, *Geophys. Res. Lett., 8,* 173, 1981.

Bell, A. R., The acceleration of cosmic rays in shock fronts, 1, *Mon. Not. R. Astron. Soc., 182,* 147, 1978*a*.

Bell, A. R., The acceleration of cosmic rays in shock fronts, 2, *Mon. Not. R. Astron. Soc., 182,* 443, 1978*b*.

Bernstein, W., R. W. Fredricks, and F. L. Scarf, A model for a broad, disordered transition between the solar wind and the magnetosphere, *J. Geophys. Res., 69,* 1201, 1964.

Blandford, R. R., and J. P. Ostriker, Particle acceleration by astrophysical shocks, *Astrophys. J., 221,* L29, 1978.

Bonifazi, C., A. Egidi, G. Moreno, and S. Orsini, Backstreaming ions outside the earth's bow shock and their interaction with the solar wind, *J. Geophys. Res., 85,* 3461, 1980.

Brown, L. W., The galactic radio spectrum between 130 and 2600 kHz, *Astrophys. J., 180,* 359, 1973.

Burlaga, L., R. Lepping, R. Weber, T. Armstrong, C. Goodrich, J. Sullivan, D. Gurnett, P. Kellogg, E. Keppler, F. Mariani, F. Neubauer, H. Rosenbauer, and R. Schwenn, Interplanetary particles and fields, November 22 to December 6, 1977: Helios, Voyager, and Imp observations between 0.6 and 1.6 AU, *J. Geophys. Res., 85,* 2227, 1980.

Chen, G., and T. P. Armstrong, Particle acceleration in the interplanetary medium, 1, Numerical simulation of the motions of charged particles near interplanetary shock waves, paper presented at Panel Presentation 5 of the Conference on Solar Terrestrial

Relations, Calgary, Alberta, August 28–September 1, 1972.
Coroniti, F. V., F. L. Scarf, C. F. Kennel, E. J. Smith, and A. M. A. Frandsen, Low-frequency electromagnetic waves detected behind interplanetary shocks, submitted to *J. Geophys. Res.*, 1982.
Dryer, M., Z. K. Smith, G. H. Endrud, and J. H. Wolfe, Pioneer 7 observations of the August 29, 1966, interplanetary shock-wave ensemble, *Cosmic Electrodyn., 3,* 184, 1972.
Dryer, M., Z. K. Smith, R. S. Steinolfson, J. D. Mihalov, J. H. Wolfe, and J. K. Chao, Interplanetary disturbances caused by the August 1972 solar flares as observed by Pioneer 9, *J. Geophys. Res., 81,* 4651, 1976.
Eichler, D., Particle acceleration in collisionless shocks: Regulated injection and high efficiency, *Astrophys. J., 229,* 419, 1979.
Eichler, D., A cosmic ray mediated shock in the solar system, *Reprint AP81-029,* Univ. of Maryland Astronomy Program, College Park, 1981.
Fairfield, D. H., Bow shock associated waves observed in the far upstream interplanetary medium, *J. Geophys. Res., 74,* 3541, 1969.
Fairfield, D. H., Whistler waves observed upstream from collisionless shocks, *J. Geophys. Res., 79,* 1368, 1974.
Formisano, V., The physics of the earth's collisionless shock wave, *J. Phys., 38,* C6-65, 1977.
Fredricks, R. W., C. F. Kennel, F. L. Scarf, G. M. Crook, and I. M. Green, Detection of electric field turbulence in the earth's bow shock, *Phys. Rev. Lett., 21,* 1761, 1968.
Fredricks, R. W., G. M. Crook, C. F. Kennel, I. M. Green, and F. L. Scarf, OGO 5 observations of electrostatic turbulence in bow shock magnetic structures, *J. Geophys. Res., 75,* 3751, 1970.
Galeev, A. A., Collisionless shocks, in *Physics of Solar-Planetary Environments,* eidted by D. J. Williams, p. 464, AGU, Washington, D. C., 1976.
Gary, S. P., Microinstabilities upstream of the earth's bow shock: A brief review, *J. Geophys. Res., 86,* 4331, 1981.
Gosling, J. T., A. J. Hundhausen, and S. J. Bame, Solar wind evolution at large heliocentric distances: Experimental demonstration and the test of a model, *J. Geophys. Res., 81,* 2111, 1976.
Gosling, J. T., J. R. Asbridge, S. J. Bame, G. Paschmann, and N. Sckopke, Observations of two distinct populations of bow shock ions in the upstream solar wind, *Geophys. Res. Lett., 5,* 957, 1978.
Greenstadt, E. W. Energies of backstreaming protons in the foreshock, *Geophys. Res. Lett., 3,* 553, 1976.
Greenstadt, E. W., and R. W. Fredricks, Shock systems in collisionless plasmas, in *Solar System Plasma Physics,* vol. 3, edited by C. F. Kennel, L. J. Lanzerotti, and E. N. Parker, North-Holland, Amsterdam, 1979.
Greenstadt, E. W., M. Hoppe, and C. T. Russell, Magnetic field orientation and suprathermal ion streams in the earth's foreshock, *J. Geophys. Res., 85,* 3473, 1980.
Grigorieva, V. P., and V. I. Slysh, Long wave cosmic radio radiation in circumlunar space (in Russian), *Kosm. Issled., 8,* 284, 1970.
Gurnett, D. A., The earth as a radio source: The nonthermal continuum, *J. Geophys. Res., 80,* 2751, 1975.
Gurnett, D. A., and L. A. Frank, Ion acoustic waves in the solar wind, *J. Geophys. Res., 83,* 58, 1978.
Gurnett, D. A., F. M. Neubauer, and R. Schwenn, Plasma wave turbulence associated with interplanetary shocks, *J. Geophys. Res., 84,* 541, 1979.
Hoang, S., J.-L. Steinberg, G. Epstein, P. Tilloles, J. Fainberg, and R. G. Stone, The low-frequency continuum as observed in the solar wind from ISEE 3: Thermal electrostatic noise, *J. Geophys. Res., 85,* 3419, 1980.
Hoppe, M., C. T. Russell, L. A. Frank, T. E. Eastman, and E. W. Greenstadt, Upstream hydromagnetic waves and their association with backstreaming ion populations: ISEE 1 and 2 observtions, *J. Geophys. Res., 86,* 4471, 1981.
Intriligator, D. S., The August 1972 solar-terrestrial events: Solar wind plasma observations, *Space Sci. Rev., 19,* 629, 1976.
Kellogg, P. J., Calculation and observation of thermal electrostatic noise in solar wind plasma, submitted to *Plasma Phys.*, 1981.
Kennel, C. F., Collisionless shocks and upstream waves and particles: Introductory remarks, *J. Geophys. Res., 86,* 4325, 1981.
Kennel, C. F., and R. Z. Sagdeev, Collisionless shock waves in high β plasmas, 1, *J. Geophys. Res., 72,* 3303, 1967.
Krimsky, G. F., *Dokl. Akad. Nauk. SSR, 234,* 1306, 1977.
Lazarus, A. J., K. W. Ogilvie, and L. F. Burlaga, Interplanetary shock observations by Mariner 5 and Explorer 34, *Solar Phys., 13,* 232, 1970.
Meyer-Vernet, N., On natural noises detected by antennas in plasmas, *J. Geophys. Res., 84,* 5373, 1979.
Ness, N. F., C. S. Scearce, and J. B. Seek, Initial results of the IMP 1 magnetic field experiment, *J. Geophys. Res., 69,* 3531, 1964.
Neubauer, F. M., G. Musmann, and G. Dehmel, Fast magnetic fluctuations in the solar wind: Helios 1, *J. Geophys. Res., 82,* 3201, 1977.
Olson, J. V., R. E. Holzer, and E. J. Smith, High frequency magnetic fluctuations associated with the earth's bow shock, *J. Geophys. Res., 74,* 4601, 1969.
Parker, E. N., A quasilinear model of plasma shock structure in a longitudinal magnetic field, *J. Nucl. Energy Part C, 2,* 146, 1961.
Parks, G. K., E. W. Greenstadt, C. S. Wu, C. S. Lin, A. St-Marc, R. P. Lin, K. A. Anderson, C. Gurgiolo, B. Mauk, H. Reme, R. R. Anderson, and T. Eastman, Upstream particle spatial gradients and plasma waves, *J. Geophys. Res., 86,* 4343, 1981.
Paschmann, G., N. Sckopke, S. J. Bame, J. R. Asbridge, J. T. Gosling, C. T. Russell, and E. W. Greenstadt, Association of low-frequency waves with suprathermal ions in the upstream solar wind, *Geophys. Res. Lett., 6,* 209, 1979.
Pesses, M. E., On the acceleration of energetic protons by interplanetary shock waves, Ph.D. thesis, Univ. of Iowa, Iowa City, 1979.
Pesses, M. E., R. B. Decker, and T. P. Armstrong, The acceleration of charged particles in interplanetary shock waves, *Preprint JHU/APL 80-10,* Johns Hopkins Applied Physics Laboratory, Laurel, Md., 1980.
Podgorny, I. M., Collisionless shocks: Simulation and laboratory experiments, *Nuovo Cimento, 2C,* 1979.
Rodriguez, P., Magnetosheath electrostatic turbulence, *J. Geophys. Res., 84,* 917, 1979.
Rodriguez, P., and D. A. Gurnett, Electrostatic and electromagnetic turbulence associated with the earth's bow shock, *J. Geophys. Res., 80,* 19, 1975.
Scarf, F. L., Wave-particle phenomena associated with shocks in the solar wind, *Proceedings of the De Feiter Memorial Symposium on the Study of Traveling Interplanetary Phenomena,* D. Reidel, Hingham, Mass., 1978.
Scarf, F. L., W. Bernstein, and R. W. Fredricks, Electron acceleration and plasma instabilities in the transition region, *J. Geophys. Res., 70,* 9, 1965.
Scarf, F. L., R. W. Fredricks, L. A. Frank, C. T. Russell, P. J. Coleman, Jr, and M. Neugebauer, Direct correlations of large-amplitude waves with suprathermal protons in the upstream solar wind, *J. Geophys. Res., 75,* 7316, 1970.
Scarf, F. L., R. W. Fredricks, L. A. Frank, and M. Neugebauer, Nonthermal electrons and high frequency waves in the upstream solar wind, 1, Observations, *J. Geophys. Res., 76,* 5162, 1971.
Scarf, F. L., R. W. Fredricks, I. M. Green, and G. M. Crook, Observations of interplanetary plasma waves, spacecraft noise, and sheath phenomena on IMP 7, *J. Geophys. Res., 79,* 73, 1974.
Scarf, F. L., R. W. Fredricks, D. A. Gurnett, and E. J. Smith, The ISEE-C plasma wave investigation, *IEEE Trans. Geosci. Electron., GE-16,* 191, 1978.
Scarf, F. L., D. A. Gurnett, and W. S. Kurth, The first year of Voyager plasma wave observations in the solar wind, *Proceedings Solar Wind Four Conference,* Springer-Verlag, Berlin, in press, 1981.
Scholer, M., F. M. Ipavich, G. Gloeckler, D. Hovestadt, and B. Klecker, Upstream particle events close to the bow shock and 200 R_E upstream: ISEE 1 and ISEE 3 observations, *Geophys. Res. Lett., 7,* 73, 1980.
Schwenn, R., M. D. Montgomery, H. Rosenbauer, H. Miggenrieder, K. H. Mulhauser, S. J. Bame, W. C. Feldman, and R. T. Hansen, Direct observations of the latitudinal extent of a high-speed stream in the solar wind, *J. Geophys. Res., 83,* 1011, 1978.
Schwenn, R., K. H. Mulhauser, and H. Rosenbauer, Two states of the solar wind at the time of solar activity minimum, 1, Boundary layers between fast and slow streams, in *Lecture Notes in Physics,* Springer, New York, in press, 1980.
Sentman, D. D., C. F. Kennel, and L. A. Frank, Plasma rest-frame distributions of suprathermal ions in the earth's foreshock region, *J. Geophys. Res., 86,* 4365, 1981*a*.
Sentman, D. D., J. P. Edmiston, and L. A. Frank, Low-frequency

parallel propagating electromagnetic instabilities in the earth's foreshock region, *J. Geophys. Res., 86,* in press, 1981*b*.

Shabanskii, V. P., Particle acceleration by passage of a hydromagnetic shock wave front, *Sov. Phys. JETP, 14,* 791, 1962.

Smith, E. J., and J. H. Wolfe, Pioneer 10, 11 observations of evolving solar wind streams and shocks beyond 1 AU, in *Study of Traveling Interplanetary Phenomena,* edited by M. A. Shea, D. F. Smart, and S. T. Wu, p. 228, D. Reidel, Hingham, Mass., 1977.

Smith, E. J., and J. H. Wolfe, Fields and plasmas in the outer solar system, *Space Sci. Rev., 23,* 217, 1979.

Sonnerup, B. U. O., Acceleration of particles reflected at a shock front, *J. Geophys. Res., 74,* 1301, 1969.

Terasawa, T., Energy spectrum and pitch angle distribution of particles reflected by MHD shock waves of fast mode, *Planet. Space Sci., 27,* 193, 1979*a*.

Terasawa, T., Origin of 30–100 keV protons observed in the upstream region of the earth's bow shock, *Planet. Space Sci., 27,* 365, 1979*b*.

Vaisberg, O. L., and G. N. Zastenker, Solar wind and magnetosheath observations at earth during August 1972, *Space Sci. Rev., 19,* 687, 1976.

Weber, R. R., J. Fainberg, and R. G. Stone, Low frequency radio observations of the solar wind near the moon, *Geophys. Res. Lett., 3,* 297, 1976.

Wentzel, D. G., High-speed interstellar gas dynamics: Shocks moderated by cosmic rays, *Astrophys. J., 170,* 53, 1971.

(Received December 18, 1980;
revised September 9, 1981;
accepted September 10, 1981.)